Cell Reports

Article

Analgesic targets identified in mouse sensory neuron somata and terminal pain translatomes

Graphical abstract

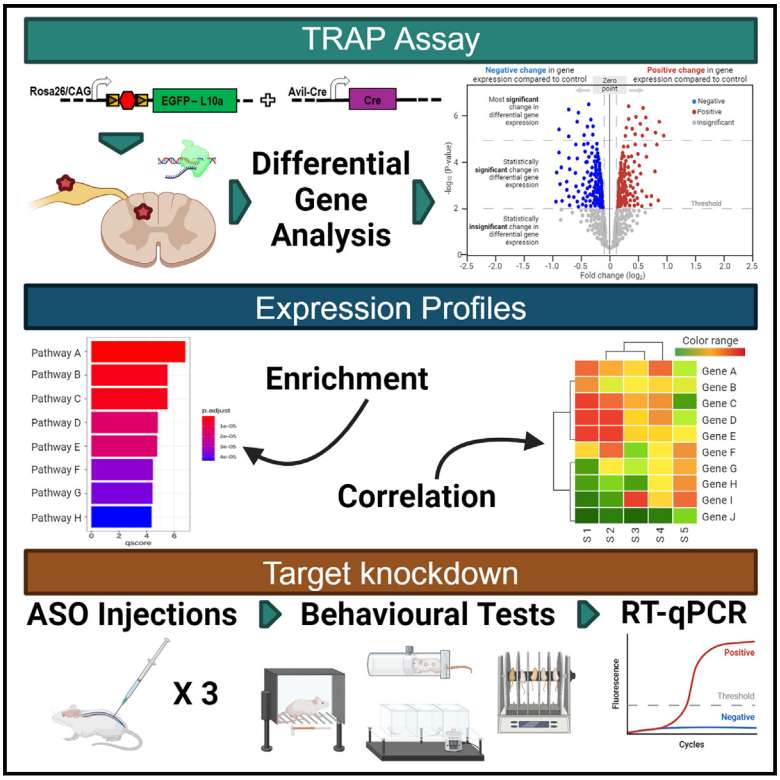

Highlights

- TRAP was used to find polysome-associated mRNA in mouse DRG somata and central terminals
- Pain-free, normal, and pain states produce different mRNA expression profiles
- Somata and terminal translatomes show significant differences
- Translational knockdown of some pain-induced genes results in pain relief

Authors

M. Ali Bangash, Cankut Cubuk, Federico Iseppon, ..., Myles J. Lewis, John N. Wood, Jing Zhao

Correspondence

j.wood@ucl.ac.uk (J.N.W.), jing02.zhao@ucl.ac.uk (J.Z.)

In brief

Bangash et al. adapted translating ribosome affinity purification technology to examine polysome-associated transcripts in both somata and central terminals of dorsal root ganglion neurons and identify potential candidates involved in pain pathways. They find that translational knockdown of *Gnas*, *Nos1ap*, *Necab2*, *Ube2f*, and *Thoc7* significantly alter pain thresholds in mice.

Bangash et al., 2024, Cell Reports *43*, 114614
August 27, 2024
https://doi.org/10.1016/j.celrep.2024.114614

CellPress

Cell Reports

CellPress
OPEN ACCESS

Article

Analgesic targets identified in mouse sensory neuron somata and terminal pain translatomes

M. Ali Bangash,[1,3] Cankut Cubuk,[2,3] Federico Iseppon,[1,3] Rayan Haroun,[1] Chloe Garcia,[1] Ana P. Luiz,[1] Manuel Arcangeletti,[1] Samuel J. Gossage,[1] Sonia Santana-Varela,[1] James J. Cox,[1] Myles J. Lewis,[2] John N. Wood,[1,4,*] and Jing Zhao[1,*]

[1]Molecular Nociception Group, Wolfson Institute for Biomedical Research, University College London WC1E 6BT, UK
[2]Centre for Experimental Medicine and Rheumatology, William Harvey Research Institute, Barts and The London School of Medicine and Dentistry, Queen Mary University of London, London EC1M 6BQ, UK
[3]These authors contributed equally
[4]Lead contact
*Correspondence: j.wood@ucl.ac.uk (J.N.W.), jing02.zhao@ucl.ac.uk (J.Z.)
https://doi.org/10.1016/j.celrep.2024.114614

SUMMARY

The relationship between transcription and protein expression is complex. We identified polysome-associated RNA transcripts in the somata and central terminals of mouse sensory neurons in control, painful (plus nerve growth factor), and pain-free conditions (Nav1.7-null mice). The majority (98%) of translated transcripts are shared between male and female mice in both the somata and terminals. Some transcripts are highly enriched in the somata or terminals. Changes in the translatome in painful and pain-free conditions include novel and known regulators of pain pathways. Antisense knockdown of selected somatic and terminal polysome-associated transcripts that correlate with pain states diminished pain behavior. Terminal-enriched transcripts included those encoding synaptic proteins (e.g., synaptotagmin), non-coding RNAs, transcription factors (e.g., Znf431), proteins associated with transsynaptic trafficking (HoxC9), GABA-generating enzymes (Gad1 and Gad2), and neuropeptides (Penk). Thus, central terminal translation may well be a significant regulatory locus for peripheral input from sensory neurons.

INTRODUCTION

Sensory neurons are essential to drive almost all pain conditions, so their biology is of keen interest for analgesic drug development. Sensory neuron-specific transcripts,[1] mRNA transcriptional profiles,[2,3] and proteomic studies[4,5] have been used to examine sensory neurons in control and pain states. Distinct rather than common sets of transcriptional responses are hallmarks of different pain stimuli,[2] suggesting that a number of mechanisms drive pain from the periphery. RNA sequencing (RNA-seq) is often used to characterize sensory neurons but may miss low-abundance RNAs.[6] In addition, transcription is not necessarily coupled to protein translation, and mRNA levels are not sufficient to predict protein concentrations.[7] In cells as large as sensory neurons, with processes of up to a meter in length in humans, protein synthesis does not only occur in somata. Axonal protein synthesis has been observed,[8] while presynaptic protein synthesis in CNS neurons has been causally related to neurotransmitter release.[9] The control of mRNA transport from soma to terminals is complex and incompletely understood.[10]

The central terminals of sensory neurons are a key regulatory site in pain pathways, as exemplified by Nav1.7-null mutant mice, where deficits in the central terminals lead to loss of neurotransmitter release, resulting in a pain-free phenotype.[11,12] Thus defining which proteins are selectively translated in sensory neuron terminals is potentially important and provides information that is not revealed by transcriptional analysis. In this study, we have used the technique of immunoprecipitating polysomes that are actively engaged in protein synthesis, so that we can identify ribosome-associated mRNAs in dorsal root ganglion (DRG) sensory neurons. Translating ribosome affinity purification (TRAP) exploits an epitope tagged (eGFP-L10) ribosomal protein as a target for antibodies that enable translating polysomes to be isolated.[13,14] This approach has been used to examine somatic translatomes in sensory neurons in neuronal injury[15] and neuropathic pain.[16] These studies have also shown potential sexual dimorphism in prostaglandin signaling from somatic sensory translatomes.[17]

We modified the somatic TRAP method (see STAR Methods) to enable specific enrichment and isolation of ribosome-bound actively translating mRNAs from both the somata and the central terminals of sensory neurons. We coupled the TRAP method with a DRG-specific Cre recombinase, using advillin (Adv)-Cre to enable DRG neuron-specific eGFP tagging of sensory neuron ribosomes. This enables isolation of actively translating mRNAs from both sensory neuronal somata and central terminals. We asked whether the translatome was gender specific, and if it changed in painful or pain-free conditions. We used nerve growth factor (NGF) to lower pain thresholds and

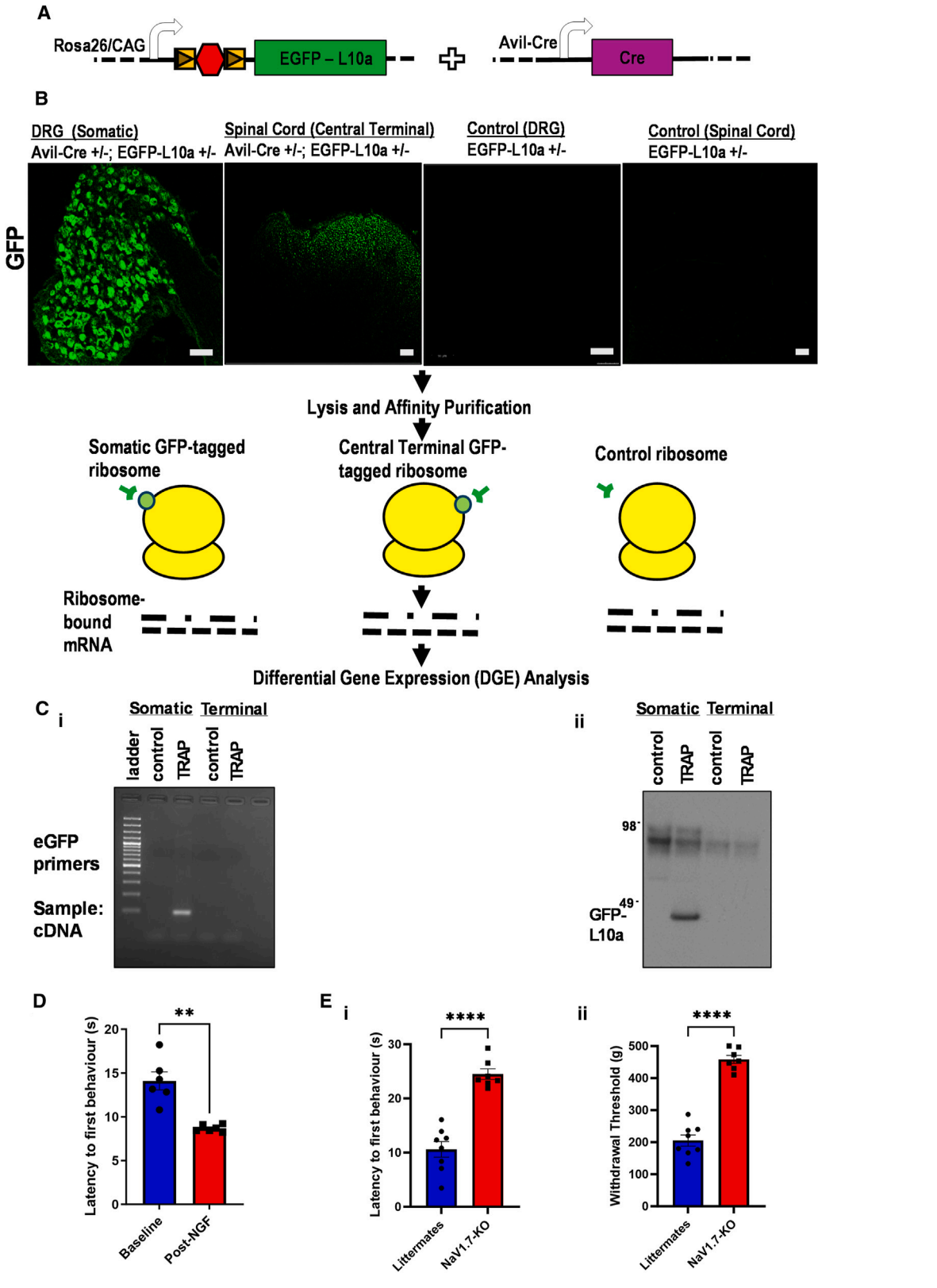

(legend on next page)

the Nav1.7 knockout mouse as a pain-free mouse model to examine pain-related alterations in translated proteins. We examined some identified pain-related transcripts using antisense oligonucleotides (ASOs) to block translation to test any significant role in pain behavior. Here, we describe the somatic and terminal translatome of mice and define known and novel analgesic targets involved in pain pathways identified with TRAP technology.

RESULTS

The technology employed to define ribosome-associated transcripts in the somata and terminals of sensory neurons is described in Figure 1. In order to isolate mRNAs translated in soma and central terminals of DRG neurons, we used the eGFP-L10 line,[18] in which Cre-mediated recombination activated expression of the 60S ribosomal subunit, L10a (RPL10a) tagged to eGFP. We crossed the eGFP-L10a line with the Adv-Cre line, which expresses Cre in all DRG sensory neurons (Figure 1A), permanently labeling the ribosomes in both somata and central terminals with GFP.[19] We sought to visualize tagged ribosomes using immunocytochemistry with GFP antibodies, detecting GFP in both the DRG soma and central terminals in the spinal cord (Figure 1B), confirming TRAP can label ribosomes in central DRG synapses. We confirmed the somatic ribosomal labeling with GFP using RT-PCR (Figure 1Ci) and immunoblotting using GFP antibodies (Figure 1Cii). The mRNA bound to ribosomes represents a very small fraction of total mRNA, especially so in the central terminals, and GFP-L10a levels from spinal cord were, thus, below the detection level of immunoblotting (Figure 1Cii), while the lack of an RT-PCR signal in terminal samples suggests that the ribosomal subunits are not themselves translated in the terminals but originate in the soma.

In order to assess the level of background mRNA non-specifically binding to immunoglobulins, beads, or protein L, we examined the signal from eGFP-L10a lines without Cre, detecting no GFP signal (Figures 1B, 1Ci, and 1Cii) and detecting negligible amounts of total mRNA immunoprecipitated from these Cre-negative samples. Therefore, the immunoprecipitation (IP) of GFP-tagged ribosomal-mRNA complexes from dissected DRG and spinal cord seems to reflect polysome-associated mRNA in these samples.

We needed to generate mice in different pain states, and we selected Adv-Cre floxed Nav1.7-null mutant mice as pain-free examples,[12] as well as normal mice treated with NGF as a model for inflammatory pain (Figures 1D and 1E).[20]

Sex-specific translatomes?

We analyzed somatic ribosome-bound mRNAs (the translatome) from dissected DRGs from Adv-Cre-GFPL10a mice using RNA-seq. We compared male Adv-Cre; eGFPL10a samples directly with female samples (Figure 2A). The alternative method of normalizing the TRAP IP (translatome) to the unbound supernatant ("transcriptome")[14] is likely to dilute the sensory neuron translatome because the unbound fraction from a heterogeneous tissue such as the spinal cord or DRG will contain many non-neuronal mRNAs.

The potential problem of low-level contamination of RNA transcripts in our TRAP samples is to some extent obviated by the fact that concentrating on high read number altered transcripts in different protocols is likely to reflect specific IP profiles. We sequenced 20,480 genes from somatic male and female Adv-Cre; eGFPL10a DRGs, out of which 460 were differentially expressed (Figures 2A and 2B and Table S1).

Since TRAP isolates ribosome-bound mRNAs in a cell-type-specific manner, we tested the specificity of our TRAP IP by examining the expression of non-neuronal DRG genes (e.g., *GFAP*) and found them to be completely absent from IP samples (Figure 2E). This confirms the specificity of the TRAP pull-down. We have listed all sequenced genes with read counts, fold changes, log2 fold changes, and *p* values in a series of supplementary tables that link to each of the volcano figures (Figure S1 and Tables S1, S2, and S3).

Adv-Cre; eGFPL10a somatic and terminal translatomes are shared by male and female mice

Despite the low abundance of ribosome-bound mRNA in central terminals of DRGs, we were able to successfully isolate and sequence the terminal translatome from pooled dissected spinal cords from Adv-Cre; eGFPL10a mice (Figure 2B). Although we sequenced a higher number of low-read-number genes in the terminal compared to the somatic TRAP, this likely represented a higher background from the greater mass of spinal cord tissue.

Comparing male and female DRG sensory neuron total translatomes directly, we identified a small fraction of sex-specific transcripts (116 of 20,480 genes), indicating predominantly shared pain pathways including key pain genes (Figures 2C and 2D). We tested the specificity of our terminal IP by examining the expression of non-neuronal DRG genes (for example GFAP) and postsynaptic dorsal horn neuronal genes (for example PDYN absent in normal DRG neurons[21]), which were found to be entirely absent in our transcriptome datasets (Figure 2E).

The vast majority (>98%) of the translatome was shared between male and female mice suggesting predominantly shared pain mechanisms, including key pain genes (e.g., *Scn9a* and

Figure 1. TRAP strategy for polysome isolation and sequencing

(A) Generation of Adv-Cre-eGFPL10 mice. eGFP L10 mice with an upstream floxed stop sequence were mated with Adv-Cre mice to generate DRG-specific GFP-tagging of ribosomes.

(B) Somatic and central terminal TRAP strategy: immunocytochemistry of DRG and spinal cord slices showing GFP-tagged ribosomal expression using polyclonal anti-GFP antibody. Scale bar: 50 μm. Tagged ribosomes were affinity purified using monoclonal anti-GFP antibodies before DGE analysis.

(C) RT-PCR detection (i) and immunoblotting (ii) of GFP-tagged ribosomes from somatic and central terminal lysates.

(D) NGF-evoked increased pain sensitivity was measured using the Hargreaves' test in both male and female mice.

(E) The acute pain-free status of Adv-Cre Nav1.7-null mice was confirmed with measurements of thermal (i) and mechanical (ii) thresholds. Mean latencies in (D) were compared using two-tailed paired t test, while mean latencies and withdrawal thresholds in (E) were compared using two-tailed unpaired t test. $^{**}p < 0.01$; $^{****}p < 0.0001$. See Table S6.

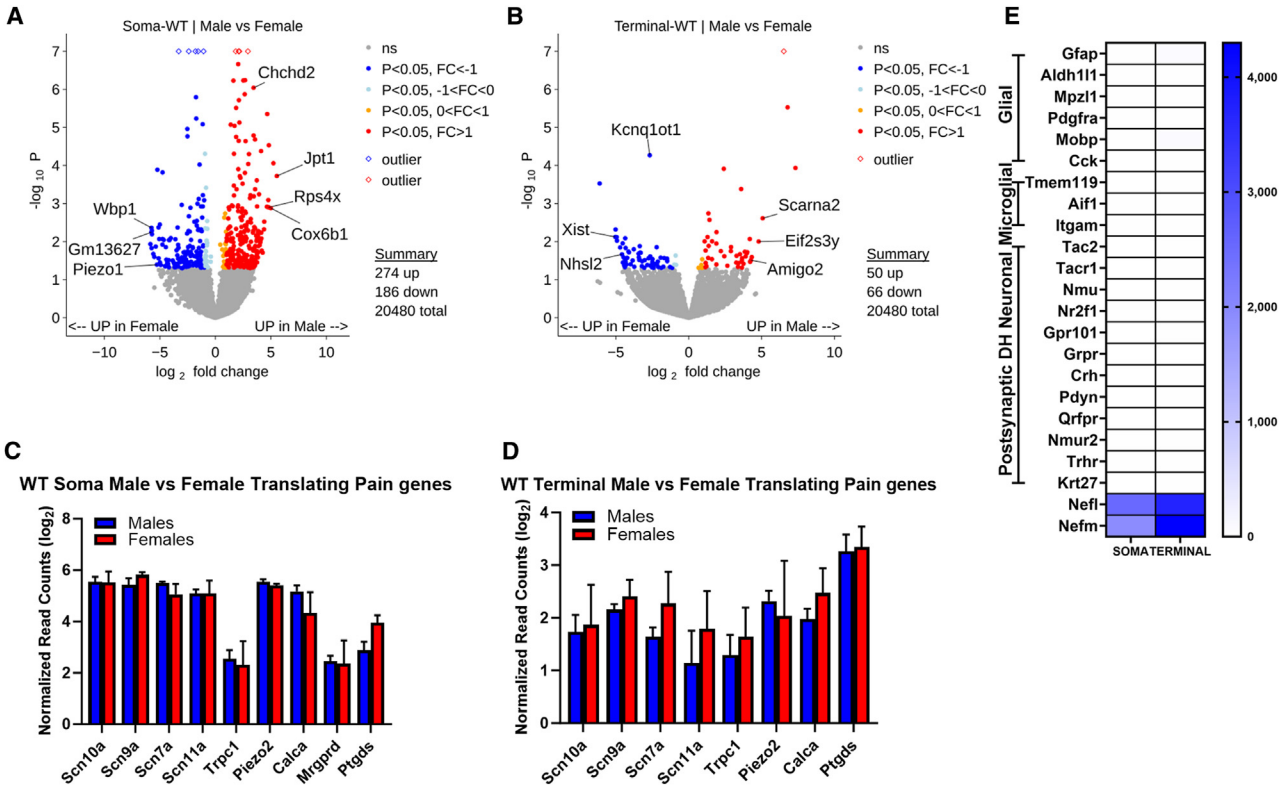

Figure 2. Sex differences in male and female translatomes

(A) Volcano plot showing differentially expressed translated genes in the soma between male ($n = 6$) and female ($n = 6$) samples. Statistical analysis by Wald test using DESeq2. Genes on the left side of the plot are upregulated in females, and upregulated male genes are shown on the right side. Non-significant genes are shown in gray, significant genes ($p < 0.05$) with $\log_2$ fold change <1 with blue, and significant genes with $\log_2$ fold change >1 are represented with red color. The x axis and y axis show $\log_2$ fold change and $-\log_{10} p$ value, respectively. Complete data comprising read numbers and fold increase ($\log_2$) with p values are presented in Excel format in Table S1.

(B) Same as in (A), but the volcano plot shows the genes expressed in the terminals. Complete data comprising read numbers and fold increase ($\log_2$) with p values are presented in Excel format in Table S1. A volcano plot showing pooled data from somata and terminals is detailed in Figure S1.

(C) Bar plot comparing the expression levels of known pain genes in male (in blue) and female (in red) somata.

(D) Bar plot comparing the expression levels of known pain genes in male (in blue) and female (in red) terminals.

(E) Heatmap showing the log read counts of different non-neuronal genes. The expression of these genes is very low when compared to control genes (Nefl and Nefm) expressed at similar levels in translatomes of soma and terminals. Normalized read counts in (C) and (D) were compared using unpaired t test. See Table S6.

Scn10a) (Figure 2C and Table S1). These numbers are consistent with recent TRAP-seq studies,[15,16] including a study of sex differences from TRAP samples in Nav1.8+ neurons.[17] In total DRG neuronal samples, we found a small increase in *Ptgds* mRNA in female mouse somata with low read numbers (see Table S1) consistent with the data in Tavares-Ferreira et al.[17]

When comparing somatic male and female translatome data, we found that *Piezo1*, a mechanosensitive channel, was upregulated in females, although transcript levels were low. In female terminals, *Kcnq1ot1* is 8-fold enriched; this is a long ncRNA that is known to interact with chromatin.[22] Intriguingly *Xist*, which is totally absent from somatic translatomes, is found in central terminals and enriched in female mice.[23] This gene, crucial for X inactivation, may associate with polysomes like other ncRNAs, but its mechanisms of action remain uncertain. *Nhsl2* is a cytoplasmic calcium-binding protein 20-fold upregulated in females that is linked to Nance-Horan syndrome.[24]

In male somata, the gene *Chchd2* implicated in stress responses to low oxygen was upregulated 20-fold with high read numbers,[25] while *Jpot1*, which encodes a nuclear envelope protein, was 50-fold upregulated. Very interestingly, the mRNA encoding the isoform of ribosomal protein RPS4X is 30-fold enriched in the male translatome, suggesting that there is a potential for gender-specific differences in ribosomal composition at the terminals.[26]

The top genes differentially upregulated in male terminals include the translational control gene *Eif2s3y*,[26] which is 30-fold upregulated in males and is known to enhance synaptic efficacy in male but not female mice. Its overexpression is linked to autism.[22] *Scarna2* is an ncRNA that has multiple functions in DNA repair and is 30-fold upregulated in males, while *Amigo2* has been implicated in synaptic function and cell-cell interactions and is 20-fold upregulated in males.[27]

Taken together, the results support the claim that terminal translatome transcripts accurately reflect transcripts present in

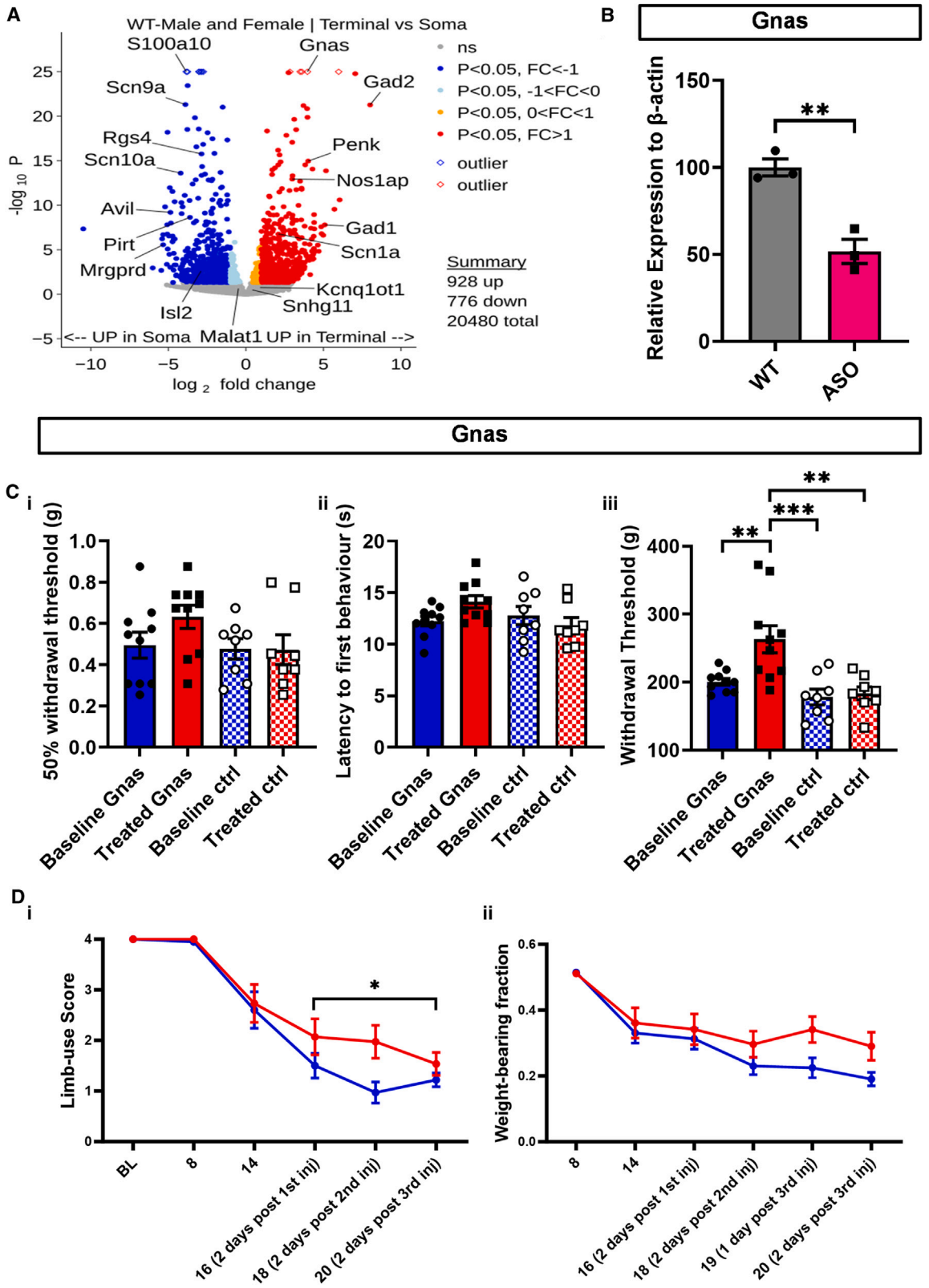

(legend on next page)

sensory neurons but generally absent from other cell types (Table S1). The fact that major pain-related genes are shared by male and female mice led us to focus on male mice to minimize animal usage.

Distinct translatomes in somata and terminals

Although 90% of transcripts were common to terminal and soma translatomes, and those present at very low read levels potentially included some contaminating material, about 5% of transcripts were enriched either in the soma or in the terminals (1,704 genes from a total of 20,480 examined), with some more than 30-fold (Figures 3 and S2 and Table S2). There were some interesting findings. For example, *Penk* mRNA encoding the enkephalins was substantially enriched in the terminals and absent from the soma, a finding consistent with recent insights into opioid signaling within the spinal cord and regulation of pain pathways.[12] In contrast, calcitonin gene-related peptide genes were principally translated in the soma, perhaps because these peptides play an important role at the peripheral terminal in regulating blood flow.[28] Voltage-gated sodium channels are a topic of interest for pain studies, and Nav1.1 was enriched in the terminals of sensory neurons, while Nav1.7, Nav1.8, and the key regulator of Nav1.8 expression, p11 (S100A10), were substantially enriched in somatic polysomes.[29] Enzymes associated with the production of GABA (Gad1 and Gad2) were enriched in the translatome with high read numbers.[30] The complete data are to be found in the supplementary tables, and potential functions are debated in the discussion.

We investigated the role of some peripherally enriched transcripts using antisense knockdown. *Nos1ap* has been linked to neuropathic pain in global knockout studies.[31] It is also implicated in neuropathic pain in mice, and some progress has been made in developing blockers of interactions with NOS. Our data suggest that terminal *Nos1ap* plays a role in pain induction (Figure S3). *Gnas* is an interesting and complex imprinted gene that encodes the alpha subunit of the adenyl cyclase activating complex Gs. Gain-of-function mutations in *GNAS* are associated with painful conditions in humans.[32] We found a clear inhibition of thermal and mechanical acute pain with ASOs directed against *Gnas* delivered intrathecally, while scrambled control ASOs were inactive (Figure 3C), correlating with a knockdown of *Gnas* mRNA Figure 3B. Given the role of adenyl cyclases in inflammatory pain, this is an interesting potential target for localized pain therapies. To further check this hypothesis, we tested the knockdown of *Gnas* in a mouse model of cancer-induced bone pain using three intrathecal injections of ASOs against *Gnas* (Figure 3D). The knockdown of this gene resulted in a modest reduction of pain-like behavior associated with this model, as assessed by limb use scoring and weight-bearing. Statistical analyses indicated that the knockdown of *Gnas* expression slowed down the reduction of the limb use significantly compared to control mice (Figure 3Di). While the improvement of weight-bearing following *Gnas* knockdown was apparent, it failed to reach the 0.05 level of statistical significance (Table S6). For these antisense experiments, motor coordination was measured with a rotarod apparatus, and no impairment was observed (Figures S4A and S4B). It is likely that our antisense protocols will diminish both transcript levels as well as the translation of candidate target genes. Nevertheless, if there is less mRNA to translate, this approach still relates to the role of the translatome in regulating pain pathways.

The TRAP RNA-seq data not only identified protein-coding mRNAs but also a significant number of non-coding RNAs that were associated with the sensory neuron ribosomes.[33] This is consistent with previous polysome profiling data where it was found that the majority (70%) of cytoplasmic expressed long non-coding (lnc) RNAs have more than half of their cytoplasmic copies associated with polysomal fractions.[33] Whether the sensory neuron polysome-associated lncRNAs identified here actively participate in regulating translation, or have other ribosomal functions, in different pain states merits further investigation.

NGF-induced pain states alter translatome activity

In order to address potential alterations in the translatome in pain states, we used the well-characterized inflammatory mediator NGF to sensitize mouse tissues globally (Figure 1D). We then used TRAP technology to compare the polysome-associated transcripts in an NGF-evoked pain state with normal mice (Table S3). A number of studies have examined translational alterations in NGF-evoked pain states in mice, but these events do not seem to be mirrored in the polysome-associated transcripts that we identified.[34]

NGF acting through TrkA is known to sensitize pain pathways at the level of sensory neuron activation. We examined the

Figure 3. Somatic versus terminal translatomes

(A) Volcano plot showing differentially expressed translated genes between somata (n = 6) and terminal (n = 6) samples. Genes on the left side of the plot are upregulated in somata, and upregulated terminal genes are shown on the right side. Non-significant transcripts are gray, significant genes ($p < 0.05$) with log2 fold change <1 are blue, and significant genes with $\log_2$ fold change >1 are represented with a red color. The x axis and y axis show $\log_2$ fold change and $-\log_{10} p$ value, respectively. Complete data comprising read numbers and fold increase ($\log_2$) with p values are presented in Table S2. Further comparisons between somata and terminal genes, as well as gene enrichment pathways in both conditions, are detailed in Figure S1.

(B) Histogram showing the antisense oligonucleotide (ASO) knockdown of the *Gnas* transcript in the spinal cord terminals by quantitative RT-PCR (n = 3). The mRNA expression levels are normalized to the housekeeping gene β-actin.

(C) Antisense oligonucleotide (ASO) knockdown of *Gnas* significantly lowers mechanical pain sensitivity. Mice (n = 10) were tested with the von Frey (i), Hargreaves' (ii), and Randall-Selitto (iii) tests before (baseline) and after ASO intrathecal injection (treated) and further compared with another set of mice (n = 8) treated with scrambled control ASOs (ctrl).

(D) Cancer-induced bone pain is attenuated by lowering translation of Gnas. Both limb use (i) and weight-bearing (ii) improved after ASO knockdown of Gnas mRNA (red) compared to controls (blue). Motor impairment tests for (C) are shown in Figure S4. Mean mRNA expression levels in (B) were compared using two-tailed Student's t test. Mean latencies and withdrawal thresholds in (C) were compared using one-way ANOVA with multiple comparison tests. Limb scores and weight-bearing fractions in (D) were compared using restricted maximum likelihood analysis (REML). *$p < 0.05$; **$p < 0.01$; ***$p < 0.001$. See Table S6.

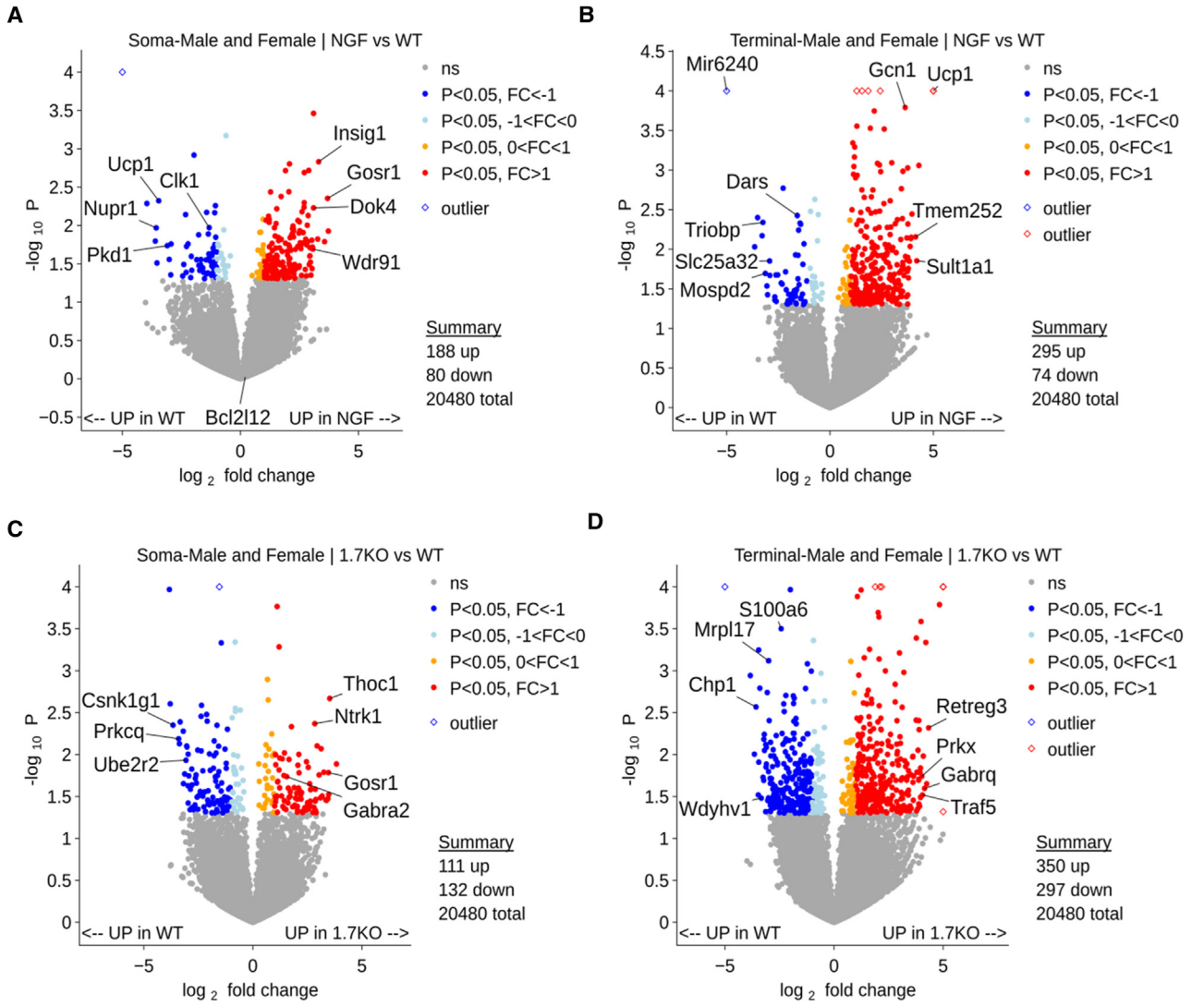

Figure 4. NGF-induced transcripts in somatic and terminal translatomes

(A) Volcano plots showing differentially expressed translated genes between NGF-enriched (n = 6) and control (n = 6) samples in the somata.
(B) Volcano plots showing differentially expressed translated genes between NGF-enriched (n = 6) and control (n = 6) samples in the terminals.
(C) Volcano plots showing differentially expressed translated genes between Nav1.7-null (n = 6) and control (n = 6) samples in the somata.
(D) Volcano plots showing differentially expressed translated genes between Nav1.7-null (n = 6) and control (n = 6) samples in the terminals. DESeq2 was used for statistical analysis. Genes on the left side of the plot are downregulated by NGF and NGF-upregulated genes are shown on the right side. Non-significant genes are in gray, significant genes ($p < 0.05$) with $\log_2$ fold change <1 are blue, and significant genes with $\log_2$ fold change >1 are represented with red color. The x axis and y axis show $\log_2$ fold change and $-\log_{10}$ p value, respectively. Complete data comprising read numbers and fold increase (with $\log_2$) with p values are presented in Excel format in Table S3. Histograms detailing the gene enrichment pathways in all conditions are shown in Figures S5 and S6.

alterations in the soma and terminals comparing NGF-treated samples with control samples. We found 268 genes of 20,480 examined were dysregulated in the soma, while more changes (369 transcripts) were altered in the terminal from the 20,480 examined (Figure 4).

A range of mRNAs were upregulated in the somatic translatome on NGF treatment (Figure 4A). These included mitochondrial proteins that could be involved in increased metabolic activity in activated sensory neurons, *Unc79*, which encodes the mouse homolog of UNC79,[35] which is a subunit of the sodium ion leak channel NALCN, and *Dok4*, a transmembrane tyrosine kinase receptor involved in regulating neurite outgrowth during nervous system development.[36]

In terminals (Figure 4B), we found that *Gcn1*, whose encoded protein enhances translation by removing stalled ribosomes and is associated with polysomes, was strongly upregulated, consistent with increased protein synthesis.[37] Other enhanced transcripts included phenol sulfotransferase *Sult1a1,*[38] whose human homolog is highly inducible by dopamine and is part of a family of proteins thought to protect neurons from neurotoxicity,[39] as well as*Tmem252*, thought to play a possible role in kidney function.[40] Bioinformatic

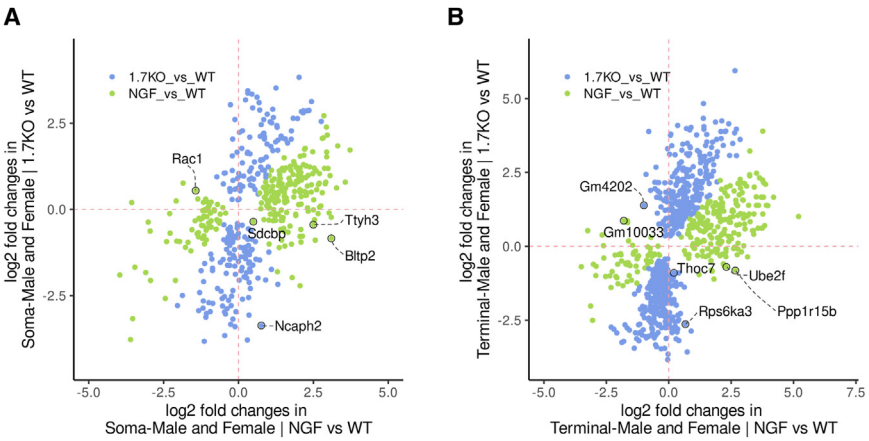

Figure 5. Differences in gene expression between NGF-treated and Nav1.7-null mice soma and terminals

Scatterplots showing differentially expressed translated genes between Nav1.7-null ($n = 6$) and NGF-treated ($n = 6$) samples in the somata (A) and terminals (B). Non-significant genes are not shown; significant genes ($p < 0.05$) in the NGF vs. wild type comparison are shown in green, whereas significant genes ($p < 0.05$) in the 1.7 null vs. wild type comparison are shown in blue. The x axis and y axis show $\log_2$ fold change for the two comparisons. Complete data comprising read numbers and fold increase ($\log_2$) with p values are presented in Excel format in Table S3. Histograms detailing the gene enrichment pathways in both conditions are shown in Figure S7.

analysis links enhanced glutamatergic synapse activity as well as PI3 kinase Akt signaling activity with the terminals to NGF-induced enhanced pain states—in agreement with such enhanced activity found in the spinal cord in chronic pain (Figure S5).[41]

Pain-free Nav1.7-null mouse translatomes

We examined the alteration in translatomes in the pain-free Nav1.7-null mouse (Figure 4 and Table S3). Among genes downregulated in the somatic translatome are several that were not detected in microarray analysis of Nav1.7-null DRG.[2] Genes shown in Figure 4 could be potential mediators in pain pathways. 132 genes were downregulated in soma, and 557 were lower in terminals of pan-DRG pain-free Nav1.7-null mice.

Among the genes downregulated in Nav1.7-null somata (Figure 4C), the *Clock* gene is a bHLH transcription factor that controls the expression of the Per genes that in DRG regulate neuronal excitability with a circadian rhythm.[42] *Mrgprd* is a GPCR that is activated by enkephalins and other ligands.[43] Protein kinase C theta (*Prkcq*) is a calcium-independent serine-threonine kinase involved in neurotransmitter release.[44] Tyrosine hydroxylase (*Th*) generates dopamine from tyrosine that then gives rise to catecholamines, all of which are implicated in pain regulation. Casein kinase 1 gamma 1 (*Csnk1g1*) phosphorylates acidic proteins on serine and threonine and has been linked to epilepsy.[45]

Within the terminals (Figure 4D), transcripts reduced in the Nav1.7-null mice translatome include *Ppp6r1*, a phosphatase that may be involved in nuclear factor κB signaling.[46] *Mepce* is involved in RNA methylation and enhances Pol2 dependent transcription.[47]

Tssc4 is a tumor suppressor implicated in a large range of pathologies.[48] *Chp1* is a key component of the Na/H exchanger and is a calcium-binding EF hand protein.[49] Inflammatory pain as well as intracellular pH control are linked to these proteins. *Hhipl1* is a hedgehog-interacting protein linked to morphogenesis and differentiation.[50]

Bioinformatic analysis shows diminished glutamatergic and dopaminergic synapse activity in Nav1.7 nulls, and oxidative phosphorylation genes are also downregulated in both somata and terminals in the pain-free state (Figure S6). This fits with less sensory neuron activity in the absence of nociceptive input.

Identifying translated proteins that correlate with pain states

Now that we had the repertoires of translated genes in pain-free and painful states from somata and terminals of DRG sensory neurons (Figure 5), we were able to focus on translated genes that correlate strongly with enhanced pain and examine their potential significance using antisense knockdown behavioral assays.

We examined the relative expression of promising candidate genes in pain states, in the pain-free mouse, and the wild-type controls to select potential targets for antisense experiments. Volcano plots are shown in Figure 4 and scatterplots in Figure 5, where a number of potential targets are identified. Bioinformatic analysis of pain-related transcripts identified in this analysis is presented in Figure S7.

We compared expression of some of the most promising candidate genes in the somata of mice as shown in Figure 6A, where the relative expression is color-coded. We found some transcripts were present at very low levels in both pain-free and normal mice but highly expressed with NGF (e.g., *Wdr91*[51] and *Cav2*), while others showed a gradation of increased expression that correlated with enhanced pain states (e.g., *Sdcbp*[52] and *Rgs4*[53]) (Figure 6B). *Sdcbp* or syntenin is associated with kainate receptor expression, while the *Necab* family of genes are neuronal specific,[52] and *Necab2* is associated with mGlu receptors linked to autism and neurodegeneration.[54,55] Sensory neuron glutamate receptors have been implicated in altered pain states. *Ttyh3*, a chloride channel, has been implicated in epilepsy, chronic pain, and viral infections.[56] Related channels have been reported to form Ca^{2+}- and cell volume-regulated anion channels structurally distinct from any characterized protein family with potential roles in cell adhesion, migration, and developmental signaling. *Wdr91* is implicated in neurodegeneration and lysosome function.[51] *Psme3* activates the proteosome,[57] while *Cav2* is a caveolin-like molecule of unknown function. *Mtmr3* or myotubularin-related protein regulates the cell cycle.[58] *Ncaph2* is implicated in cognitive decline and

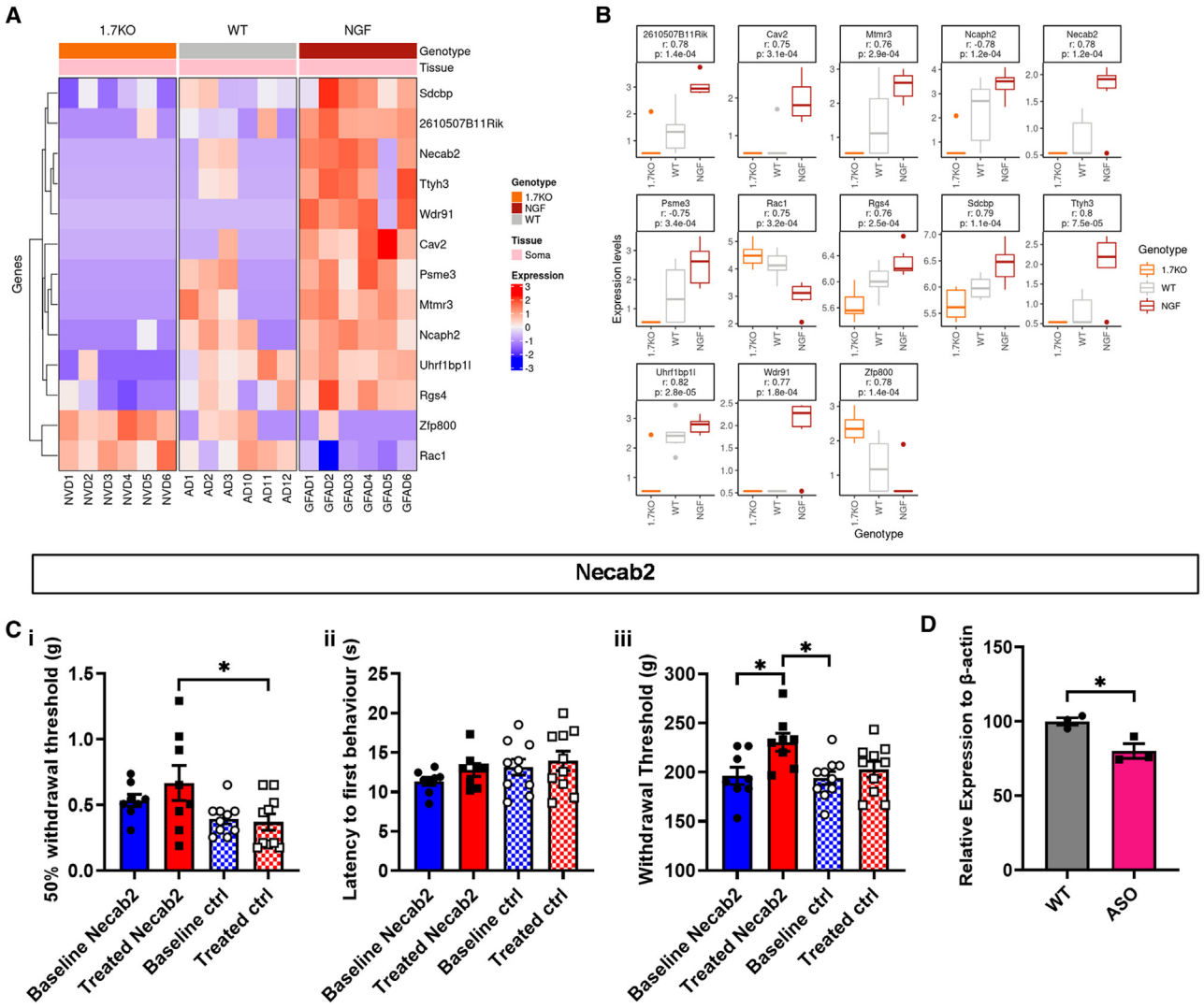

Figure 6. Pain-related somatic transcripts and effects of transcript ASO knockdown on acute pain behavior

(A) Color-coded levels of expression in individual mice (abscissa) for transcripts that show a level of ribosome association with enhanced pain levels.

(B) Relative levels of expression of transcripts shown in (A) derived from Table S3, together with Pearson's correlation coefficient and the respective *p* value of the correlation.

(C) Antisense oligonucleotide (ASO) knockdown of Necab2 significantly lowers mechanical pain sensitivity. Mice ($n = 8$) were tested with the von Frey (i), Hargreaves' (ii), and Randall-Selitto (iii) tests before (baseline, blue) and after ASO intrathecal injection (treated, red) and compared with another set of mice ($n = 10$) treated with generic scrambled control ASOs.

(D) Histogram showing the antisense oligonucleotide (ASO) knockdown of the Necab2 transcript in the DRGs by quantitative RT-PCR ($n = 3$). The expression levels are normalized to the housekeeping gene β-actin. Motor impairment tests for (C) are shown in Figure S7. Mean latencies and withdrawal thresholds in (C) were compared using one-way ANOVA with multiple comparison tests. Mean mRNA expression levels in (D) were compared using two-tailed Student's t test. $^{*}p < 0.05$; $^{**}p < 0.01$. See Table S6.

Alzheimer's disease,[59] while *Rgs4* is linked to schizophrenia and G protein function. *Rac1* is a small GTPase linked to the inflammasome,[60] and *Uhrf1bp11* is a lipid transfer bridge.[61]

Sdcbp, a syndecan-binding protein, shows an excellent translational correlation with enriched expression after NGF treatment and lower expression in Nav1.7-null mice;[62] *Ttyh3*,[47] a large conductance calcium-activated chloride channel, presents high expression in NGF-treated mice and is absent in $Na_V1.7$ nulls, while *Wdr91*, a negative regulator of the PI3 kinase activity, is selectively translated only after NGF-dependent pain induction.

We examined the effect of ASOs delivered intrathecally directed against the single target *Necab2*, which is NGF induced and absent in pain-free samples (Figures 6C and 6D). This protein is a neuronal calcium-binding protein that binds to and modulates the function of two or more receptors, including adenosine A(2A) receptors and metabotropic glutamate receptor type 5, that are implicated in pain pathways. The inhibition of *Necab2*

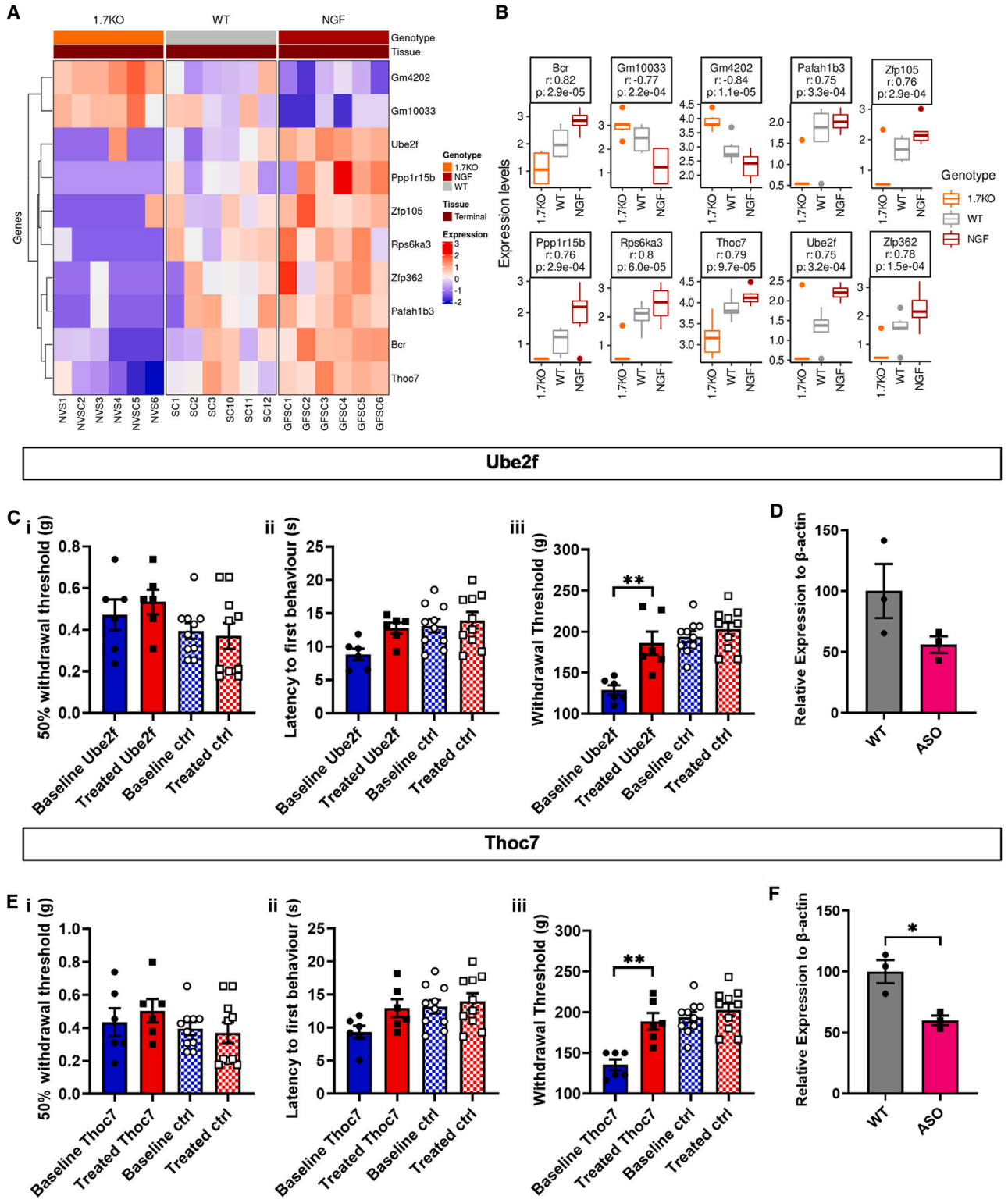

Figure 7. Pain-related central terminal transcripts and effects of transcript ASO knockdown on acute pain behavior

(A) Color-coded levels of expression in individual mice (abscissa) for transcripts that show polysome association correlating with enhanced pain levels.

(B) Relative levels of expression of transcripts shown in (A) derived from Table S3, together with Pearson's correlation coefficient and the respective *p* value of the correlation.

(legend continued on next page)

expression resulted in a diminution in noxious mechanosensation as measured with the Randall-Selitto apparatus, with no effect on heat sensing. Scrambled controls (Figure 6C) were inactive.

Changes in TRAP data from cell bodies contrast with changes in central terminals, where proteins synthesized may be expected to play some role in interactions with spinal cord neurons and central pain pathways (Table S3). Once again, we exploited color-coded tables to summarize interesting transcripts that show pain-related expression. Two uncharacterized transcripts, *Gm4202* and *Gm10033*, showed an inverse correlation to pain and were not further investigated. *Zfp105* (ZNF35) is a retinoic acid-regulated transcription factor.[63] *Rps6ka3* is a member of the ribosomal 6 kinase family that plays a wide-ranging role in signal transduction.[64] BCR is a GTPase-activating protein that also acts on tyrosine kinases. *Thoc7* has an important role in RNA translocation from the nucleus as well as viral release.[65]

We examined antisense knockdown of transcripts like *Thoc7* that show a pain correlation in terms of local protein synthesis (Figure 7). Another terminally translated protein investigated was *Ube2f*, a ubiquitin-conjugating enzyme involved in neddylation that is known to play a role in pain pathways and to stabilize voltage-gated sodium channel activity. Interestingly, *Ppp1r15b* is regulated by glutamate receptor activity that controls its kinase or phosphatase inhibitory activity.[66] Intriguingly, this protein can control the activity of *Eif2*, a key control for local translation. Lastly, *Zfp362* is assumed to be a transcription factor. *Pafah1b3* removes an acetyl group from PAF: its function is uncertain, but it seems to have a key role in brain development.[67]

Knockdown of Ube2*f* showed a significant reduction of both mechanical and thermal sensitivity across the battery of tests used, highlighting even more their potential role in pain pathways (Figures 7C and 7D). Scrambled controls were inactive. *Thoc7* showed a significant increase in mechanical thresholds when using the Randall-Selitto apparatus (Figures 7E and 7F). For these antisense experiments, motor coordination was measured with a rotarod apparatus, and no impairment was observed (Figures S4C and S4D).

DISCUSSION

Pain pathways depend on sensory neuron neurotransmitter input into the central nervous system evoked by damaging stimuli. The molecular organization of the first synapse is incompletely understood and mainly relies on immunocytochemical studies. Protein synthesis is finely regulated at several stages, from transcription to translation and trafficking. Single-cell RNA-seq has given helpful insights into cellular diversity and function, but there are limitations including the inability to detect low-level transcripts, altered transcripts during circadian changes, and further changes caused by isolation of single cells from their normal milieu. Unfortunately, proteomic analysis is relatively insensitive, making single-cell proteomic analysis at present problematic. There are thus significant gaps in our knowledge of the structure of the central terminals of sensory neurons and potential changes that may occur in acute or chronic pain states. One interesting element in the physiology of sensory neurons is the existence of local protein synthesis at axon terminals. We have adapted the TRAP technology developed by Liu et al.[18] to examine proteins synthesized both in cell bodies and at the central terminals that may have a role in synaptic function. By comparing polysome-associated transcripts in pain states with those in normal or pain-free states, we have identified several mRNAs that could play a role in pain pathways. Interestingly, there is no obvious link between the translatome and the transcriptome in the somata of sensory neurons.[7] Similarly, the mechanism and signals that result in mRNA translocation are poorly understood.[68] There are no obvious consensus 5′ or 3′ UTR sequences linked to central terminal polysome-associated transcripts. We have used bioinformatic tools to classify genes that are coordinately regulated in response to altered pain states. These data are presented in Figures S2 and S5–S7.

A broad range of transcripts have been identified in this TRAP analysis, including data that suggest the vast majority of translatome transcripts are common to male and female mice. ncRNAs are also present. These polysome-associated lncRNAs frequently have long "pseudo" 5′ UTRs and are 5′ capped, features that are important for ribosomal engagement and also nonsense-mediated decay.[33,69,70] For the majority of known ribosome-associated lncRNAs, it is still unclear whether they are engaged by the ribosomes for translation (e.g., producing short/micro peptides),[71–73] help to regulate protein translation,[74–77] inertly reside in ribosomes, or are degraded by the ribosome as a mechanism to control the cellular lncRNA population.[33] However, for some specific lncRNAs, their translation regulation function is known. For example, lincRNA-p21 associates with polysomes and suppresses the translation of JUNB and CTNNB1 mRNAs.[75] In contrast, the natural antisense transcript to ubiquitin carboxy-terminal hydrolase L1 (AS-Uchl1) promotes the translation of Uchl1 by base pairing with its sense gene at a SINEB2 element and helps associate the sense mRNA with the active translating polysome.[74]

(C) Antisense oligonucleotide (ASO) knockdown of Ube2f effects on pain sensitivity. Mice (n = 6) were tested with the von Frey (i), Hargreaves' (ii), and Randall-Selitto (iii) tests before (baseline, blue) and after ASO intrathecal injection (treated, red) and compared with another set of mice (n = 10) treated with generic scrambled control ASOs.

(D) Histogram showing the antisense oligonucleotide (ASO) knockdown of the Ube2f transcript in dorsal root ganglia by quantitative RT-PCR (n = 3). The expression levels are normalized to the housekeeping gene β-actin.

(E) Antisense oligonucleotide (ASO) knockdown of Thoc7 effects on pain sensitivity. Mice (n = 6) were tested with the von Frey (i), Hargreaves' (ii), and Randall-Selitto (iii) tests before (baseline, blue) and after ASO intrathecal injection (treated, red) and compared with another set of mice (n = 10) treated with generic scrambled control ASOs.

(F) Histogram showing the antisense oligonucleotide (ASO) knockdown of the Thoc7 transcript in the spinal cord terminals by quantitative RT-PCR (n = 3). The expression levels are normalized to the housekeeping gene β-actin. Motor impairment tests for (C) and (E) are shown in Figure S4. Mean latencies and withdrawal thresholds in (C) and (E) were compared using one-way ANOVA with multiple comparison tests. Mean mRNA expression levels in (D) and (F) were compared using two-tailed Student's t test. *$p < 0.05$; **$p < 0.01$. See Table S6.

Genes that seem to play a role in pain pathways include a range of functional proteins. Mitochondrial genes that may play a role in the increased activity found in active sensory neurons signaling pain states have been identified (e.g., COX; see Figure S6). Other interesting transcripts that are clearly involved in pain pathways (e.g., *Penk*) show no altered levels of translatome association.[78] The rate of translation of polysome-associated genes may be regulated by kinase and phosphatases acting on eukaryotic initiation factors like EIF2, and such enzymes (e.g., *Ppp1r15b*) are also present in the central translatome, so relative read counts may not give a complete picture of effective translation.[56]

Bioinformatic analysis (Figures S5 and S7) shows that enhanced pain leads to more activity of genes involved in oxidative phosphorylation and synaptic vesicle activity, as one would suspect if sensory neurons were more actively signaling in pain states.

One striking observation is the presence of transcription factors in the central terminal translatome. *HoxC9* has been proposed to shuttle across membranes,[79] and other terminal Hox genes (e.g., *Hoxc8*) are implicated in motor neuron specification. It is an intriguing possibility that Hox proteins translated at sensory neuron terminals could exert functional effects on motor neurons.[80]

We have used ASOs to examine a role for some of the translatome mRNAs in acute pain and provide evidence that some do indeed contribute to pain states. These reagents may diminish mRNA levels in general rather than those associated with polysomes, but the net effect of diminishing protein production should be the same. We first checked two terminally enriched candidates, the G protein regulatory protein *Gnas* and the nitric oxide synthase regulatory protein *Nos1ap*, both of which seem to play a role in acute pain. The novel genes that have so far not been linked to pain pathways were identified by correlating expression with enhanced pain states. Within the soma, we found regulators of kainate receptor expression (*Sdcbp*) as well as metabotropic glutamate receptors (*Necab2*).[45,46] A novel unique anion channel potentially activated by calcium (*Ttyh3*) was also identified as well as *Cav2*, a caveolin-like protein of unknown function. Both *Wdr91* and *Ncaph2* are implicated in neurodegeneration, while *Uhrf1bp1l* is a lipid transfer bridge, and *Psme3* activates the proteosome. *Rgs4* regulates G protein signaling and is a schizophrenia risk factor gene. *Rac1* is linked to innate immunity and the inflammasome, while *Zfp362* is a potential transcription factor without activity in acute pain. Table S3 contains complete rank-ordered lists of altered genes with *p* values and read counts.

Our functional studies demonstrate a clear role in acute pain for the terminally enriched transcripts *Gnas* and *Nos1Ap*, Thoc7, which regulates RNA transport, and *Ube2f*, which regulates neddylation, which are also linked to pain. Scrambled ASO controls, both targeted and general, showed no effect on pain behavior. Within the soma, *Necab2* was a strong candidate that showed a major effect on mechanical pain. With the current availability of targeted delivery systems and advances in gene therapy, these targets are worthy of further study in other models of human chronic pain. In the future, it would be helpful to appraise more complex pain states like chronic inflammatory and neuropathic pain with the substantial number of candidate genes identified, but in the interest of minimizing animal suffering, candidates that have some genetic links to human pain (e.g., *Ttyh3*) should be prioritized.

STAR★METHODS

Detailed methods are provided in the online version of this paper and include the following:

- KEY RESOURCES TABLE
- RESOURCE AVAILABILITY
  - Lead contact
  - Materials availability
  - Data and code availability
- EXPERIMENTAL MODEL AND STUDY PARTICIPANT DETAILS
  - Animals
  - Generation of eGFP-L10a mice
- METHOD DETAILS
  - Translating ribosome affinity purification (TRAP)
  - Reverse transcriptase (RT)- qPCR
  - Immunohistochemistry
  - Immunoblotting
  - RNA-seq analysis
  - Pathway analysis
  - Cancer-induced bone pain
- QUANTIFICATION AND STATISTICAL ANALYSIS

SUPPLEMENTAL INFORMATION

Supplemental information can be found online at https://doi.org/10.1016/j.celrep.2024.114614.

ACKNOWLEDGMENTS

We acknowledge with gratitude the following sources of funding: Versus Arthritis UK (21950), Medical Research Council (MR/V012509/1; 571476), and Cancer Research UK (185341). This work acknowledges the support of the National Institute for Health Research Barts Biomedical Research Centre (NIHR 203330). The views expressed are those of the authors and do not represent those of the NHS, NIHR, or funding bodies.

AUTHOR CONTRIBUTIONS

Conceptualization, M.A.B., J.Z., and J.N.W.; formal analysis, C.C. and M.J.L.; investigation, M.A.B., F.I., A.P.L., C.G. M.A., R.H., S.J.G., and S.S-V.; resources, F.I., R.H., S.J.G., and S.S.-V.; data curation, C.C.; visualization, F.I., C.C., and M.A.B.; writing – original draft, J.N.W., J.Z., C.C., and F.I.; writing – review and editing, F.I., R.H., J.J.C., M.J.L., J.Z., and J.N.W.; supervision, J.N.W., J.Z., and M.J.L.; funding acquisition, J.N.W. and M.J.L.

DECLARATION OF INTERESTS

The authors declare no competing interests.

Received: November 20, 2023
Revised: June 7, 2024
Accepted: July 24, 2024
Published: August 19, 2024

REFERENCES

1. Akopian, A.N., and Wood, J.N. (1995). Peripheral nervous system-specific genes identified by subtractive cDNA cloning. J. Biol. Chem. *270*, 21264–21270.

2. Bangash, M.A., Alles, S.R.A., Santana-Varela, S., Millet, Q., Sikandar, S., de Clauser, L., Ter Heegde, F., Habib, A.M., Pereira, V., Sexton, J.E., et al. (2018). Distinct transcriptional responses of mouse sensory neurons in models of human chronic pain conditions. Wellcome Open Res. *3*, 78. https://doi.org/10.12688/wellcomeopenres.14641.1.

3. LaCroix-Fralish, M.L., Austin, J.S., Zheng, F.Y., Levitin, D.J., and Mogil, J.S. (2011). Patterns of pain: meta-analysis of microarray studies of pain. Pain *152*, 1888–1898. https://doi.org/10.1016/j.pain.2011.04.014.

4. Kanellopoulos, A.H., Koenig, J., Huang, H., Pyrski, M., Millet, Q., Lolignier, S., Morohashi, T., Gossage, S.J., Jay, M., Linley, J.E., et al. (2018). Mapping protein interactions of sodium channel NaV1. 7 using epitope-tagged gene-targeted mice. The EMBO journal *37*, 427–445.

5. Huang, H.-L., Cendan, C.-M., Roza, C., Okuse, K., Cramer, R., Timms, J.F., and Wood, J.N. (2008). Proteomic profiling of neuromas reveals alterations in protein composition and local protein synthesis in hyper-excitable nerves. Mol. Pain *4*, 33.

6. Usoskin, D., Furlan, A., Islam, S., Abdo, H., Lönnerberg, P., Lou, D., Hjerling-Leffler, J., Haeggström, J., Kharchenko, O., Kharchenko, P.V., et al. (2015). Unbiased classification of sensory neuron types by large-scale single-cell RNA sequencing. Nat. Neurosci. *18*, 145–153. https://doi.org/10.1038/nn.3881.

7. Schmidt, M., Sondermann, J.R., Gomez-Varela, D., Çubuk, C., Millet, Q., Lewis, M.J., Wood, J.N., and Zhao, J. (2022). Transcriptomic and proteomic profiling of NaV1. 8-expressing mouse nociceptors. Front. Mol. Neurosci. *15*, 1002842.

8. Shigeoka, T., Koppers, M., Wong, H.H.W., Lin, J.Q., Cagnetta, R., Dwivedy, A., de Freitas Nascimento, J., van Tartwijk, F.W., Ströhl, F., Cioni, J.M., et al. (2019). On-Site Ribosome Remodeling by Locally Synthesized Ribosomal Proteins in Axons. Cell Rep. *29*, 3605–3619.e10. https://doi.org/10.1016/j.celrep.2019.11.025.

9. Scarnati, M.S., Kataria, R., Biswas, M., and Paradiso, K.G. (2018). Active presynaptic ribosomes in the mammalian brain, and altered transmitter release after protein synthesis inhibition. Elife *7*, e36697. https://doi.org/10.7554/eLife.36697.

10. Sahoo, P.K., Lee, S.J., Jaiswal, P.B., Alber, S., Kar, A.N., Miller-Randolph, S., Taylor, E.E., Smith, T., Singh, B., Ho, T.S.-Y., et al. (2018). Axonal G3BP1 stress granule protein limits axonal mRNA translation and nerve regeneration. Nat. Commun. *9*, 3358.

11. MacDonald, D.I., Sikandar, S., Weiss, J., Pyrski, M., Luiz, A.P., Millet, Q., Emery, E.C., Mancini, F., Iannetti, G.D., and Alles, S.R. (2020). The mechanism of analgesia in NaV1. 7 null mutants. Preprint at bioRxiv. 2020.2006.2001.127183.

12. MacDonald, D.I., Sikandar, S., Weiss, J., Pyrski, M., Luiz, A.P., Millet, Q., Emery, E.C., Mancini, F., Iannetti, G.D., Alles, S.R.A., et al. (2021). A central mechanism of analgesia in mice and humans lacking the sodium channel NaV1. 7. Neuron *109*, 1497–1512.e6.

13. Heiman, M., Schaefer, A., Gong, S., Peterson, J.D., Day, M., Ramsey, K.E., Suárez-Fariñas, M., Schwarz, C., Stephan, D.A., Surmeier, D.J., et al. (2008). A translational profiling approach for the molecular characterization of CNS cell types. Cell *135*, 738–748.

14. Doyle, J.P., Dougherty, J.D., Heiman, M., Schmidt, E.F., Stevens, T.R., Ma, G., Bupp, S., Shrestha, P., Shah, R.D., Doughty, M.L., et al. (2008). Application of a translational profiling approach for the comparative analysis of CNS cell types. Cell *135*, 749–762.

15. Rozenbaum, M., Rajman, M., Rishal, I., Koppel, I., Koley, S., Medzihradszky, K.F., Oses-Prieto, J.A., Kawaguchi, R., Amieux, P.S., Burlingame, A.L., et al. (2018). Translatome Regulation in Neuronal Injury and Axon Regrowth. eNeuro *5*. https://doi.org/10.1523/ENEURO.0276-17.2018.

16. Megat, S., Ray, P.R., Moy, J.K., Lou, T.F., Barragán-Iglesias, P., Li, Y., Pradhan, G., Wanghzou, A., Ahmad, A., Burton, M.D., et al. (2019). Nociceptor Translational Profiling Reveals the Ragulator-Rag GTPase Complex as a Critical Generator of Neuropathic Pain. J. Neurosci. *39*, 393–411. https://doi.org/10.1523/JNEUROSCI.2661-18.2018.

17. Tavares-Ferreira, D., Ray, P.R., Sankaranarayanan, I., Mejia, G.L., Wangzhou, A., Shiers, S., Uttarkar, R., Megat, S., Barragan-Iglesias, P., Dussor, G., et al. (2022). Sex Differences in Nociceptor Translatomes Contribute to Divergent Prostaglandin Signaling in Male and Female Mice. Biol. Psychiatry *91*, 129–140. https://doi.org/10.1016/j.biopsych.2020.09.022.

18. Liu, J., Krautzberger, A.M., Sui, S.H., Hofmann, O.M., Chen, Y., Baetscher, M., Grgic, I., Kumar, S., Humphreys, B.D., Hide, W.A., and McMahon, A.P. (2014). Cell-specific translational profiling in acute kidney injury. J. Clin. Invest. *124*, 1242–1254.

19. Santana-Varela, S., Bogdanov, Y.D., Gossage, S.J., Okorokov, A.L., Li, S., De Clauser, L., Alves-Simoes, M., Sexton, J.E., Iseppon, F., Luiz, A.P., et al. (2021). Tools for analysis and conditional deletion of subsets of sensory neurons. Wellcome Open Res. *6*, 250.

20. Barker, P.A., Mantyh, P., Arendt-Nielsen, L., Viktrup, L., and Tive, L. (2020). Nerve growth factor signaling and its contribution to pain. J. Pain Res. *13*, 1223–1241.

21. Nguyen, E., Lim, G., Ding, H., Hachisuka, J., Ko, M.-C., and Ross, S.E. (2021). Morphine acts on spinal dynorphin neurons to cause itch through disinhibition. Sci. Transl. Med. *13*, eabc3774.

22. Zhang, M., Zhou, Y., Jiang, Y., Lu, Z., Xiao, X., Ning, J., Sun, H., Zhang, X., Luo, H., Can, D., et al. (2021). Profiling of sexually dimorphic genes in neural cells to identify Eif2s3y, whose overexpression causes autism-like behaviors in male mice. Front. Cell Dev. Biol. *9*, 669798.

23. Schwämmle, T., and Schulz, E.G. (2023). Regulatory principles and mechanisms governing the onset of random X-chromosome inactivation. Curr. Opin. Genet. Dev. *81*, 102063.

24. Brooks, S.P., Coccia, M., Tang, H.R., Kanuga, N., Machesky, L.M., Bailly, M., Cheetham, M.E., and Hardcastle, A.J. (2010). The Nance–Horan syndrome protein encodes a functional WAVE homology domain (WHD) and is important for co-ordinating actin remodelling and maintaining cell morphology. Hum. Mol. Genet. *19*, 2421–2432.

25. Zhou, Z.-D., Saw, W.-T., and Tan, E.-K. (2017). Mitochondrial CHCHD-containing proteins: physiologic functions and link with neurodegenerative diseases. Mol. Neurobiol. *54*, 5534–5546.

26. Zinn, A.R., Alagappan, R.K., Brown, L.G., Wool, I., and Page, D.C. (1994). Structure and function of ribosomal protein S4 genes on the human and mouse sex chromosomes. Molecular and cellular biology *14*, 2485–2492.

27. Soto, F., Tien, N.-W., Goel, A., Zhao, L., Ruzycki, P.A., and Kerschensteiner, D. (2019). AMIGO2 scales dendrite arbors in the retina. Cell Rep. *29*, 1568–1578.e4.

28. Goodman, E.C., and Iversen, L.L. (1986). Calcitonin gene-related peptide: novel neuropeptide. Life Sci. *38*, 2169–2178.

29. Lischka, A., Eggermann, K., Record, C.J., Dohrn, M.F., Laššuthová, P., Kraft, F., Begemann, M., Dey, D., Eggermann, T., and Beijer, D. (2023). Genetic landscape of congenital insensitivity to pain and hereditary sensory and autonomic neuropathies. Brain *awad328*.

30. Grone, B.P., and Maruska, K.P. (2016). Three distinct glutamate decarboxylase genes in vertebrates. Sci. Rep. *6*, 30507.

31. Lee, W.-H., Li, L.-L., Chawla, A., Hudmon, A., Lai, Y.Y., Courtney, M.J., and Hohmann, A.G. (2018). Disruption of nNOS-NOS1AP protein-protein interactions suppresses neuropathic pain in mice. Pain *159*, 849–863.

32. Zhadina, M., Roszko, K.L., Geels, R.E.S., de Castro, L.F., Collins, M.T., and Boyce, A.M. (2021). Genotype-phenotype correlation in fibrous dysplasia/McCune-Albright syndrome. J. Clin. Endocrinol. Metab. *106*, 1482–1490.

33. Carlevaro-Fita, J., Rahim, A., Guigó, R., Vardy, L.A., and Johnson, R. (2016). Cytoplasmic long noncoding RNAs are frequently bound to and degraded at ribosomes in human cells. RNA *22*, 867–882. https://doi.org/10.1261/rna.053561.115.

34. Zhu, W., and Oxford, G.S. (2011). Differential gene expression of neonatal and adult DRG neurons correlates with the differential sensitization of TRPV1 responses to nerve growth factor. Neurosci. Lett. *500*, 192–196.

35. Bayat, A., Liu, Z., Luo, S., Fenger, C.D., Højte, A.F., Isidor, B., Cogne, B., Larson, A., Zanus, C., Faletra, F., et al. (2023). A new neurodevelopmental disorder linked to heterozygous variants in UNC79. Genet. Med. *25*, 100894.

36. Uchida, M., Enomoto, A., Fukuda, T., Kurokawa, K., Maeda, K., Kodama, Y., Asai, N., Hasegawa, T., Shimono, Y., Jijiwa, M., et al. (2006). Dok-4 regulates GDNF-dependent neurite outgrowth through downstream activation of Rap1 and mitogen-activated protein kinase. J. Cell Sci. *119*, 3067–3077.

37. Müller, M.B., Kasturi, P., Jayaraj, G.G., and Hartl, F.U. (2023). Mechanisms of readthrough mitigation reveal principles of GCN1-mediated translational quality control. Cell *186*, 3227–3244.e20.

38. Raftogianis, R.B., Wood, T.C., Otterness, D.M., Van Loon, J.A., and Weinshilboum, R.M. (1997). Phenol sulfotransferase pharmacogenetics in humans: association of commonSULT1A1alleles with TS PST phenotype. Biochem. Biophys. Res. Commun. *239*, 298–304.

39. Sidharthan, N.P., Minchin, R.F., and Butcher, N.J. (2013). Cytosolic sulfotransferase 1A3 is induced by dopamine and protects neuronal cells from dopamine toxicity: role of D1 receptor-N-methyl-D-aspartate receptor coupling. J. Biol. Chem. *288*, 34364–34374.

40. Zhou, X., Wang, N., Liu, W., Chen, R., Yang, G., and Yu, H. (2023). Identification of the potential association between SARS-CoV-2 infection and acute kidney injury based on the shared gene signatures and regulatory network. BMC Infect. Dis. *23*, 655.

41. Chen, S.-P., Zhou, Y.-Q., Liu, D.-Q., Zhang, W., Manyande, A., Guan, X.-H., Tian, Y.-k., Ye, D.-W., and Omar, D.M. (2017). PI3K/Akt pathway: a potential therapeutic target for chronic pain. Curr. Pharm. Des. *23*, 1860–1868.

42. Das, V., Kc, R., Li, X., Varma, D., Qiu, S., Kroin, J.S., Forsyth, C.B., Keshavarzian, A., van Wijnen, A.J., Park, T.J., et al. (2018). Pharmacological targeting of the mammalian clock reveals a novel analgesic for osteoarthritis-induced pain. Gene *655*, 1–12.

43. Dussor, G., Zylka, M.J., Anderson, D.J., and McCleskey, E.W. (2008). Cutaneous sensory neurons expressing the Mrgprd receptor sense extracellular ATP and are putative nociceptors. J. Neurophysiol. *99*, 1581–1589.

44. Osada, S.-I., Mizuno, K., Saido, T.C., Suzuki, K., Kuroki, T., and Ohno, S. (1992). A new member of the protein kinase C family, nPKC theta, predominantly expressed in skeletal muscle. Molecular and cellular biology *12*, 3930–3938.

45. Kusuda, J., Hirai, M., Tanuma, R., and Hashimoto, K. (2000). Cloning, expression analysis and chromosome mapping of human casein kinase 1 γ1 (CSNK1G1): Identification of two types of cDNA encoding the kinase protein associated with heterologous carboxy-terminal sequences. Cytogenet. Cell Genet. *90*, 298–302.

46. Ziembik, M.A., Bender, T.P., Larner, J.M., and Brautigan, D.L. (2017). Functions of protein phosphatase-6 in NF-κB signaling and in lymphocytes. Biochem. Soc. Trans. *45*, 693–701.

47. Jeronimo, C., Forget, D., Bouchard, A., Li, Q., Chua, G., Poitras, C., Thérien, C., Bergeron, D., Bourassa, S., Greenblatt, J., et al. (2007). Systematic analysis of the protein interaction network for the human transcription machinery reveals the identity of the 7SK capping enzyme. Mol. Cell *27*, 262–274.

48. Bergfort, A., Hilal, T., Kuropka, B., Ilik, İ.A., Weber, G., Aktaş, T., Freund, C., and Wahl, M.C. (2022). The intrinsically disordered TSSC4 protein acts as a helicase inhibitor, placeholder and multi-interaction coordinator during snRNP assembly and recycling. Nucleic Acids Res. *50*, 2938–2958.

49. Cottle, W.T., Wallert, C.H., Anderson, K.K., Tran, M.F., Bakker, C.L., Wallert, M.A., and Provost, J.J. (2020). Calcineurin homologous protein isoform 2 supports tumor survival via the sodium hydrogen exchanger isoform 1 in non-small cell lung cancer. Tumour Biol. *42*, 1010428320937863.

50. Holtz, A.M., Griffiths, S.C., Davis, S.J., Bishop, B., Siebold, C., and Allen, B.L. (2015). Secreted HHIP1 interacts with heparan sulfate and regulates Hedgehog ligand localization and function. J. Cell Biol. *209*, 739–757.

51. Xing, R., Zhou, H., Jian, Y., Li, L., Wang, M., Liu, N., Yin, Q., Liang, Z., Guo, W., and Yang, C. (2021). The Rab7 effector WDR91 promotes autophagy-lysosome degradation in neurons by regulating lysosome fusion. J. Cell Biol. *220*, e202007061.

52. Grootjans, J.J., Zimmermann, P., Reekmans, G., Smets, A., Degeest, G., Dürr, J., and David, G. (1997). Syntenin, a PDZ protein that binds syndecan cytoplasmic domains. Proc. Natl. Acad. Sci. USA *94*, 13683–13688.

53. Berman, D.M., Kozasa, T., and Gilman, A.G. (1996). The GTPase-activating protein RGS4 stabilizes the transition state for nucleotide hydrolysis. J. Biol. Chem. *271*, 27209–27212.

54. Canela, L., Luján, R., Lluís, C., Burgueño, J., Mallol, J., Canela, E.I., Franco, R., and Ciruela, F. (2007). The neuronal Ca2+-binding protein 2 (NECAB2) interacts with the adenosine A2A receptor and modulates the cell surface expression and function of the receptor. Mol. Cell. Neurosci. *36*, 1–12.

55. Chen, Z., Long, H., Guo, J., Wang, Y., He, K., Tao, C., Li, X., Jiang, K., Guo, S., and Pi, Y. (2022). Autism-Risk Gene necab2 Regulates Psychomotor and Social Behavior as a Neuronal Modulator of mGluR1 Signaling. Front. Mol. Neurosci. *15*, 901682.

56. Nalamalapu, R.R., Yue, M., Stone, A.R., Murphy, S., and Saha, M.S. (2021). The tweety gene family: from embryo to disease. Front. Mol. Neurosci. *14*, 672511.

57. Boulpicante, M., Darrigrand, R., Pierson, A., Salgues, V., Rouillon, M., Gaudineau, B., Khaled, M., Cattaneo, A., Bachi, A., Cascio, P., and Apcher, S. (2020). Tumors escape immunosurveillance by overexpressing the proteasome activator PSME3. OncoImmunology *9*, 1761205.

58. Wang, Z., Zhang, M., Shan, R., Wang, Y.J., Chen, J., Huang, J., Sun, L.Q., and Zhou, W.B. (2019). MTMR3 is upregulated in patients with breast cancer and regulates proliferation, cell cycle progression and autophagy in breast cancer cells. Oncol. Rep. *42*, 1915–1923.

59. Hao, S.-W., Li, T.-R., Han, C., Han, Y., and Cai, Y.-N. (2023). Associations Between Levels of Peripheral NCAPH2 Promoter Methylation and Different Stages of Alzheimer's Disease: A Cross-Sectional Study. J. Alzheimers Dis. *92*, 899–909.

60. Sander, E.E., and Collard, J.G. (1999). Rho-like GTPases: their role in epithelial cell–cell adhesion and invasion. Eur. J. Cancer *35*, 1905–1911.

61. McEwan, D.G., and Ryan, K.M. (2022). ATG2 and VPS13 proteins: molecular highways transporting lipids to drive membrane expansion and organelle communication. FEBS J. *289*, 7113–7127.

62. Lauri, S.E., Braithwaite, S.P., oise Coussen, F., Mulle, C., Dev, K.K., Coutinho, V., Meyer, G., Isaac, J.T., Collingridge, G.L., and Henley, J.M. (2003). Rapid and Differential Regulation of AMPA and Kainate Receptors at Hippocampal Mossy Fibre Synapses by PICK1 and GRIP. Neuron *38*, 673.

63. Pengue, G., Cannada-Bartoli, P., and Lania, L. (1993). The ZNF35 human zinc finger gene encodes a sequence-specific DNA-binding protein. FEBS Lett. *321*, 233–236.

64. Merienne, K., Jacquot, S., Pannetier, S., Zeniou, M., Bankier, A., Gecz, J., Mandel, J.-L., Mulley, J., Sassone-Corsi, P., and Hanauer, A. (1999). A missense mutation in RPS6KA3 (RSK2) responsible for non-specific mental retardation. Nat. Genet. *22*, 13–14.

65. Kumar, R., Palmer, E., Gardner, A.E., Carroll, R., Banka, S., Abdelhadi, O., Donnai, D., Elgersma, Y., Curry, C.J., Gardham, A., et al. (2020). Expanding clinical presentations due to variations in THOC2 mRNA nuclear export factor. Front. Mol. Neurosci. *13*, 12.

66. Kloft, N., Neukirch, C., von Hoven, G., Bobkiewicz, W., Weis, S., Boller, K., and Husmann, M. (2012). A subunit of eukaryotic translation initiation factor 2α-phosphatase (CreP/PPP1R15B) regulates membrane traffic. J. Biol. Chem. *287*, 35299–35317.

67. Escamez, T., Bahamonde, O., Tabares-Seisdedos, R., Vieta, E., Martinez, S., and Echevarria, D. (2012). Developmental dynamics of PAFAH1B subunits during mouse brain development. J. Comp. Neurol. *520*, 3877–3894.

68. Gasparski, A.N., Mason, D.E., Moissoglu, K., and Mili, S. (2022). Regulation and outcomes of localized RNA translation. Wiley Interdiscip. Rev. RNA *13*, e1721.

69. Jackson, R.J., Hellen, C.U.T., and Pestova, T.V. (2010). The mechanism of eukaryotic translation initiation and principles of its regulation. Nat. Rev. Mol. Cell Biol. *11*, 113–127. https://doi.org/10.1038/nrm2838.

70. Kurihara, Y., Matsui, A., Hanada, K., Kawashima, M., Ishida, J., Morosawa, T., Tanaka, M., Kaminuma, E., Mochizuki, Y., Matsushima, A., et al. (2009). Genome-wide suppression of aberrant mRNA-like noncoding RNAs by NMD in Arabidopsis. Proc. Natl. Acad. Sci. USA *106*, 2453–2458. https://doi.org/10.1073/pnas.0808902106.

71. Minati, L., Firrito, C., Del Piano, A., Peretti, A., Sidoli, S., Peroni, D., Belli, R., Gandolfi, F., Romanel, A., Bernabo, P., et al. (2021). One-shot analysis of translated mammalian lncRNAs with AHARIBO. Elife *10*, e59303. https://doi.org/10.7554/eLife.59303.

72. Anderson, D.M., Anderson, K.M., Chang, C.L., Makarewich, C.A., Nelson, B.R., McAnally, J.R., Kasaragod, P., Shelton, J.M., Liou, J., Bassel-Duby, R., and Olson, E.N. (2015). A micropeptide encoded by a putative long noncoding RNA regulates muscle performance. Cell *160*, 595–606. https://doi.org/10.1016/j.cell.2015.01.009.

73. Ruiz-Orera, J., Messeguer, X., Subirana, J.A., and Alba, M.M. (2014). Long non-coding RNAs as a source of new peptides. Elife *3*, e03523. https://doi.org/10.7554/eLife.03523.

74. Carrieri, C., Cimatti, L., Biagioli, M., Beugnet, A., Zucchelli, S., Fedele, S., Pesce, E., Ferrer, I., Collavin, L., Santoro, C., et al. (2012). Long non-coding antisense RNA controls Uchl1 translation through an embedded SINEB2 repeat. Nature *491*, 454–457. https://doi.org/10.1038/nature11508.

75. Yoon, J.H., Abdelmohsen, K., Srikantan, S., Yang, X., Martindale, J.L., De, S., Huarte, M., Zhan, M., Becker, K.G., and Gorospe, M. (2012). LincRNA-p21 suppresses target mRNA translation. Mol. Cell *47*, 648–655. https://doi.org/10.1016/j.molcel.2012.06.027.

76. Pecoraro, V., Rosina, A., and Polacek, N. (2022). Ribosome-Associated ncRNAs (rancRNAs) Adjust Translation and Shape Proteomes. Noncoding. RNA *8*, 22. https://doi.org/10.3390/ncrna8020022.

77. Pircher, A., Gebetsberger, J., and Polacek, N. (2014). Ribosome-associated ncRNAs: an emerging class of translation regulators. RNA Biol. *11*, 1335–1339. https://doi.org/10.1080/15476286.2014.996459.

78. Sapio, M.R., Iadarola, M.J., Loydpierson, A.J., Kim, J.J., Thierry-Mieg, D., Thierry-Mieg, J., Maric, D., and Mannes, A.J. (2020). Dynorphin and enkephalin opioid peptides and transcripts in spinal cord and dorsal root ganglion during peripheral inflammatory hyperalgesia and allodynia. J. Pain *21*, 988–1004.

79. Prochiantz, A., and Di Nardo, A.A. (2022). Shuttling Homeoproteins and Their Biological Significance. Methods Mol. Biol. *2383*, 33–44.

80. Catela, C., Chen, Y., Weng, Y., Wen, K., and Kratsios, P. (2022). Control of spinal motor neuron terminal differentiation through sustained Hoxc8 gene activity. Elife *11*, e70766.

81. Nassar, M.A., Stirling, L.C., Forlani, G., Baker, M.D., Matthews, E.A., Dickenson, A.H., and Wood, J.N. (2004). Nociceptor-specific gene deletion reveals a major role for Nav1.7 (PN1) in acute and inflammatory pain. Proc. Natl. Acad. Sci. USA *101*, 12706–12711.

82. Zhou, X., Wang, L., Hasegawa, H., Amin, P., Han, B.X., Kaneko, S., He, Y., and Wang, F. (2010). Deletion of PIK3C3/Vps34 in sensory neurons causes rapid neurodegeneration by disrupting the endosomal but not the autophagic pathway. Proc. Natl. Acad. Sci. USA *107*, 9424–9429.

83. Heiman, M., Kulicke, R., Fenster, R.J., Greengard, P., and Heintz, N. (2014). Cell type-specific mRNA purification by translating ribosome affinity purification (TRAP). Nat. Protoc. *9*, 1282–1291. https://doi.org/10.1038/nprot.2014.085.

84. Ray, P.R., Shiers, S., Caruso, J.P., Tavares-Ferreira, D., Sankaranarayanan, I., Uhelski, M.L., Li, Y., North, R.Y., Tatsui, C., Dussor, G., et al. (2023). RNA profiling of human dorsal root ganglia reveals sex differences in mechanisms promoting neuropathic pain. Brain *146*, 749–766.

85. Sierra, C., De Toma, I., and Dierssen, M. (2021). Single nucleus RNA-seq in the hippocampus of a Down syndrome mouse model reveals new key players in memory. Preprint at: bioRxiv. 2021.2011. 2018.469102

86. Minett, M.S., Quick, K., and Wood, J.N. (2011). Behavioral measures of pain thresholds. Curr. Protoc. Mouse Biol. *1*, 383–412.

87. Haroun, R., Gossage, S.J., Luiz, A.P., Arcangeletti, M., Sikandar, S., Zhao, J., Cox, J.J., and Wood, J.N. (2023). Chemogenetic Silencing of NaV1.8-Positive Sensory Neurons Reverses Chronic Neuropathic and Bone Cancer Pain in FLEx PSAM4-GlyR Mice. eneuro *10*, ENEURO.0151-23.2023.

88. Randall, L.O. (1957). A method for measurement of analgesic activity of inflamed tissue. Arch. Int. Pharmacodyn. Ther. *111*, 409–411.

89. Chaplan, S.R., Bach, F.W., Pogrel, J.W., Chung, J.M., and Yaksh, T.L. (1994). Quantitative assessment of tactile allodynia in the rat paw. J. Neurosci. Methods *53*, 55–63.

90. Hargreaves, K., Dubner, R., Brown, F., Flores, C., and Joris, J. (1988). A new and sensitive method for measuring thermal nociception in cutaneous hyperalgesia. Pain *32*, 77–88.

STAR★METHODS

KEY RESOURCES TABLE

REAGENT or RESOURCE	SOURCE	IDENTIFIER
Antibodies		
19C8 anti-EGFP	Heintz Lab; Rockefeller University	AB_2716737; Htz-GFP-19C8
19F7 anti-EGFP	Heintz Lab; Rockefeller University	AB_2716736; Htz-GFP-19F7
Alexa 488- conjugated goat anti-mouse	Invitrogen	Cat. # A32723
goat anti-rabbit IgG-HRP	Jackson Immunoresearch Labs	AB_2313567; Cat. # 111-035-003
goat anti-mouse IgG-HRP	Jackson Immunoresearch Labs	AB_2338511; Cat. # 115-035-116
Chemicals, peptides, and recombinant proteins		
rRNasin	Promega	Cat. #N2511
Superasin	Applied Biosystems	Cat. # AM2696
TRIzol	Invitrogen	Cat. # 15596026
iScript Reverse Transcription Supermix	Bio-Rad	Cat. # 1708840
SsoAdvanced Universal SYBR Green Supermix	Bio-Rad	Cat. # 1725270
Critical commercial assays		
MyOne T1 Dynabeads	Invitrogen	Cat. # 65601
RNA Nanoprep kit	Agilent	Cat. # 400753
Quant-it Ribogreen kit	Invitrogen	Cat. #R11490
Pierce BCA protein assay kit	Sigma-Aldrich	Cat. # 71285-3
Super Signal West Dura	Thermo Scientific	Cat. # 34075
SMART-Seq v4 ultra-low Input RNA Kit	Takara Bio	Cat. # 634891
Deposited data		
RNA-Seq source data	This paper	See Tables S1, S2, and S3
Raw read counts and sample annotation files	This paper, Figshare	10.6084/m9.figshare.24581349
Raw behavioral assays data	This paper, Figshare	10.6084/m9.figshare.24581349
Experimental models: Cell lines		
Lewis lung carcinoma (LL/2) cells	ATCC	CRL-1642
Experimental models: Organisms/strains		
Mouse: $Na_V1.7$ flox	Nassar et al.[81]	N/A
Mouse: Advillin Cre	Zhou et al.[82]	N/A
Mouse: NaV1.8 Cre	Nassar et al.[81]	RRID:IMSR_JAX:036564
Mouse: eGFP-L10a	Liu J et al.[18]	RRID:IMSR_JAX:024750
Oligonucleotides		
Primers for mouse genotyping	This paper	See Table S4
Antisense Oligonucleotides	This paper	See Table S5
Software and algorithms		
BBMap software v.38.94	JGI	https://jgi.doe.gov/data-and-tools/software-tools/bbtools/
R studio	R	https://rstudio.com
HiPathia v.2.10	Hipatia	http://hipathia.babelomics.org/
Prism	Graphpad	https://www.graphpad.com/
Other		
Gnas TaqMan qPCR assay kit	ThermoFisher	Mm07303258_g1
Nos1ap TaqMan qPCR assay kit	ThermoFisher	Mm01290688_m1

(*Continued on next page*)

Continued

REAGENT or RESOURCE	SOURCE	IDENTIFIER
Necab2 TaqMan qPCR assay kit	ThermoFisher	Mm00475387_m1
Ube2f TaqMan qPCR assay kit	ThermoFisher	Mm04213187_s1
Thoc7 TaqMan qPCR assay kit	ThermoFisher	Mm00481358_g1
β-Actin TaqMan qPCR assay kit	ThermoFisher	Mm01205647_g1

RESOURCE AVAILABILITY

Lead contact

- Further information and requests for resources and reagents should be directed to and will be fulfilled by the lead contact, John N. Wood (j.wood@ucl.ac.uk).

Materials availability

- This study did not generate any new unique reagents.

Data and code availability

- TRAP gene expression counts, and sample annotation files are deposited on Figshare and are publicly available as of the date of publication. Accession link is listed in the key resource table. Complete data comprising read numbers, fold increase (log_2) and p-values are presented in Table S1, S2, and S3. Raw behavioral assays data files are deposited on Fisghare and are publicly available as of the date of publication. Accession link is listed in the key resources table.
- This paper does not report original code.
- Any additional information required to reanalyse the data reported in this paper is available from the lead contact upon request.

EXPERIMENTAL MODEL AND STUDY PARTICIPANT DETAILS

Animals

All experiments were performed in compliance with the UK Animals (Scientific Procedures) Act 1986, under a Home Office project licence (PPL 413329A2). Mice were housed in a 12-h light/dark cycle with *ad libitum* provision of food and water. All mice were acclimatized for 1 week to the facility before the start of experiments. Mice were housed in individually ventilated cages (Techniplast GM500 Mouse IVC Green line) containing Lignocel bedding with a maximum of 5 adult mice per cage. All experiments were carried out using adult male and female mice. Mice were euthanized by CO_2 asphyxiation followed by cervical dislocation.

Mice in pain free and painful conditions were tested, using Nav1.7 null mutant mice generated by crossing floxed Nav1.7 with Advillin-Cre. Mice in pain were generated by systemic injection of NGF. In order to generate Nav1.7 null mutant mice with eGFP-L10, Nav1.7 KO (Adv-cre +/−; Scn9a F/F) were mated with eGFPL10 +/− mice. First generation heterozygotes (Adv-cre +/−; Scn9a F/+; eGFPL10 +/−) were then mated with Scn9a Floxed homozygous mice (Sc9a F/F) to generate Nav1.7 null mutant mice with eGFP-L10 (Adv-cre +/−; Scn9a F/F; eGFPL10 +/−).

Generation of eGFP-L10a mice

eGFP-L10a mice were obtained from the Jackson laboratory. Homozygous or Heterozygous eGFP-L10a were then crossed with either Nav1.8-cre or Adv-cre mice to obtain Cre; eGFP-L10a heterozygote mice. All experiments were performed in 8–12 weeks old male and female mice. Details of primers used for genotyping are available in Table S4.

METHOD DETAILS

Translating ribosome affinity purification (TRAP)

TRAP assay was performed as described[83] with slight modifications. Briefly, affinity matrix was prepared by incubating MyOne T1 Dynabeads (Life Technology) with biotinylated protein L and monoclonal 19C8 and 19F7 eGFP antibodies.[83] All the bilateral DRGs or Spinal Cords from 3 male or female mice were dissected on ice, pooled and homogenized in low salt buffer, followed by extraction of post-nuclear fraction at 1000 *g* spin. This fraction was then homogenized in non-denaturing 1% NP-40 buffer followed by isolation of post-mitochondrial fraction at 12000 *g* spin. GFP tagged ribosomes were then isolated by mixing the post-mitochondrial fraction with the pre-prepared affinity matrix of eGFP antibodies and beads overnight at 4°C. After washing the beads in high-salt buffer, the ribosome bound RNA was eluted and purified using RNA Nanoprep kit (Agilent). Finally, the isolated ribosomal bound RNA was quantified using Quant-it Ribogreen kit (Invitrogen). All buffers had 100 μg/ml cycloheximide (Sigma) with 10ul/ml rRNasin (Promega) and Superasin (Applied Biosystems) to inhibit RNAases, while all reactions were carried out in RNAse-free tubes (Ambion).

Reverse transcriptase (RT)- qPCR

DRGs from all the segments or spinal cords were dissected from three mice and pooled. RNA was extracted using TRIzol Reagent (Invitrogen) according to the manufacturer's instructions. Reverse transcription was performed using iScript Reverse Transcription Supermix for reverse transcriptase–qPCR following the supplied protocol by Invitrogen. Complementary DNA amplification was performed in triplicate, using SsoAdvanced Universal SYBR Green Supermix (Bio-Rad).

Immunohistochemistry

Following anesthesia, mice were *trans*-cardially perfused with PBS, followed by 4% paraformaldehyde in PBS. DRGs and spinal cord were dissected and incubated in fixative for 4h at 4°C, followed by 30% sucrose in PBS overnight at 4°C. Tissue was embedded in O.C.T. (Tissue-Tek) and snap-frozen in a dry ice/2-methylbutane bath. DRG and spinal cord cross cryosections (20μm) were collected on glass slides (Superfrost Plus, Polyscience) and stored at −80°C until further processing. For GFP-tag immunohistochemistry in DRGs and spinal cord, sections were incubated in blocking solution (4% horse serum, 0.3% Triton X-100 in PBS) for 1h at room temperature, followed by incubation in mouse anti-GFP antibody (19C8 or 19F7) diluted 1:200 in blocking solution overnight at 4°C. Following three washes in PBS, bound antibody was visualised using an Alexa 488- conjugated goat anti-mouse secondary antibody (1:1000, Invitrogen). Fluorescence images were acquired on confocal laser scanning microscope (LSM 780, Zeiss).

Immunoblotting

Proteins for immunoblots were isolated from freshly excised DRG or spinal cord followed by homogenization in RIPA lysis buffer as described previously.[4] The nuclear fraction and cell debris were removed by centrifugation at ∼20,000 *g* for 15 min at 4°C. Protein concentrations were determined with Pierce BCA protein assay kit, and then samples of 40 μg were separated on SDS–PAGE gel in Bio-Rad Mini-PROTEAN Vertical Electrophoresis Cell System and blotted to the Immobilin-P membrane (IPVH00010, Millipore) in transfer buffer (25 mM Tris–HCl, pH 8.3, 192 mM glycine, 0.1% SDS and 20% methanol) for 1 h at 100 V with a Bio-Rad transfer cell system. The membrane was blocked in blocking buffer [5% nonfat milk in PBS–Tween buffer (0.1% Tween 20 in 1× PBS)] for 1 h at room temperature and then incubated with primary antibody, anti-GFP (19C8, 1:1000) in blocking buffer overnight at 4°C. The membrane was washed three times with TBS–Tween (20 mM Tris, 150 mM NaCl, 0.1% Tween 20, pH 7.5) and then incubated with secondary antibody goat anti-mouse or goat anti-rabbit IgG-HRP (1:4,000; Jackson ImmunoResearch Laboratories) in TBS–Tween at room temperature for 2 h. Detection was performed using a Western Lightning Chemiluminescence Reagent (Super Signal Western Dura, Thermo Scientific) and exposed to BioMax film (Kodak).

RNA-seq analysis

RNA integrity of ribosome-bound mRNA samples from three replicates was assessed using RIN and DV200 scores. SMART-Seq v4 ultra-low RNA (Takara Bio) library preparation protocol was used to generate cDNA libraries and sequencing was performed on an Illumina HiSeq 2 instrument with 150 bp reads according to the manufacturer's instructions. Samples with 50M reads were sequenced using a 2 × 150-base-pair (BP) paired-end configuration. After demultiplexing, Illumina adapters and nucleotides with poor quality were trimmed using bbduk from the BBMap software v.38.94. The mouse reference genome, Gencode release v28 (GRCm39), was edited by concatenation of the eGFP sequence retrieved from https://www.ncbi.nlm.nih.gov/nuccore/EU056363.1. The reference genome indexing, read mapping and counting mapped reads were performed using the STAR aligner v.2.7.3a in the 2-pass mapping mode that allows for unbiased exon splice junction detection.

After extracting uniquely mapped read counts, the genes that showed low expression across all samples, less than 20 total counts, were discarded from our dataset and the remaining genes were used for data quality control and downstream analysis. The remaining counts were subjected to variance-stabilizing transformation (VST) and then differential expression analysis was performed between different conditions using the DESeq2 v.1.25.9 package. A Principal Component Analysis (PCA) for unsupervised projection of RNA-Seq data was performed with prcomp function in R using normalized data and PCA plots were generated using ggplot2 v.3.3.6. All the sample clusters shown in PCA plots were highly associated with biological conditions rather than technical ones. Therefore, no batch effect correction was applied. Partition of samples based on the proportion of neuronal mRNA content was assessed using 32 genes recently published by Pradipta R Ray et al.[84] The median value of these genes was used as neuronal module score and then samples were categorized into three groups (enriched, moderate and de-enriched) using the 30th and 70th percentiles of module scores. DE-Seq2 was used to calculate *p*-values (statistical analysis by negative binomial general linear model with Wald test) and $\log_2$ fold changes that were used to generate volcano plots using easylabel package v.0.2.4. Linear relationships between genes and three genotypes (1.7KO, WT, NGF/−1, 0, 1) were identified by means of Pearson's correlation using the cor.test function of the R Stats package. Results are shown for only the genes with absolute correlation coefficient >0.75 and *p*-value <0.05. Heatmaps were generated using ComplexHeatmap v.2.12.1. Pair plots demonstrating the reproducibility of the RNAseq results are shown in Figure S8.

Pathway analysis

Geneset enrichment analysis

Differentially expressed genes were used for gene set enrichment analysis. This analysis was performed with an R interface to the Enrichr database v.3.0. The hypergeometric model was used to assess whether the number of selected genes associated with a KEGG pathway was larger than expected. Pathway terms with *p*-value <0.05 were considered significant.

Differentially active pathways

The expression levels of the genes corresponding to the proteins involved in the pathways are used by the mechanistic pathway models to infer the activities of the pathways. Activities of signaling and metabolic sub-pathways were estimated using Hipathia v.2.10 and Metabolizer v.1.7.0 tools, respectively. A two-sided Wilcoxon signed-rank test was used for the statistical assessment when comparing different conditions.

Antisense Oligonucleotides

Antisense Oligonucleotides (ASOs) directed against sequences encompassing initiator methionines and polyadenylation sites of candidate mRNAs were purchased from Sigma-Aldrich. All ASOs were 20mers, HPLC purified with phosphorothioate nucleotides at the 5′ and 3′ end (see Table S5).[85]

ASOs injections

Adult C57BL/6J mice between 8 and 10 weeks were anesthetized using 2–3% Isoflurane and injected with 6 μL of two or more targeted of control antisense oligonucleotides resuspended in PBS for a total amount of 15 μg/mouse/injection via the intrathecal route using a Hamilton syringe connected to a 30G needle cannula. A pair of ASOs designed for the extremities of the mRNA were designed for each target: their sequences can be found in Table S5. The ASOs were injected on 3 days (every other day), and mice were prepared for behavioral testing immediately after the last injection.

Quantitative RT-PCR

Reverse transcription was performed using the iScript cDNA Synthesis kit (Biorad) according to the manufacturer's conditions. TaqMan real-time PCR was carried out using probes purchased from ThermoFisher. The expression level of target genes was normalized to the housekeeping Actin gene mRNA. Relative gene expression [relative quantities (RQ) value] was determined using the $2-\Delta\Delta Ct$ equation in which control samples were designated as the calibrator. All RT-PCR data are expressed as mean ± standard error of the mean (SEM) with significance indicated by $^{*}p \leq 0.05$, $^{**}p \leq 0.01$, and $^{***}p \leq 0.001$ (two-tailed Student's t-test).

Behavioral testing

All animal experiments were performed in accordance with Home Office Regulations. Observers were blinded to treatment. Animals were acclimatized to handling by the investigator and every effort was made to minimize stress during the testing. Male animals were used for experiments apart from gender comparison studies. All experiments were filmed and carried out by two independent researchers.[86] Cancer pain studies were carried out exactly as described in.[87]

Randall Selitto

The threshold for mechanonociception was assessed using the Randall Selitto test[88] Animals were restrained in a clear plastic tube. A 3 mm^2 blunt probe was applied to the tail of the animal with increasing pressure until the mouse exhibited a nocifensive response, such as tail withdrawal. The pressure required to elicit the nocifensive behavior was averaged across three trials. The cut-off was set to 500 g.

Von Frey

Punctate mechanical sensitivity was measured using the up-down method of Chaplan to obtain a 50% withdrawal threshold.[89] Mice were habituated for 1 h in darkened enclosures with a wire mesh floor. A 0.4 g von Frey filament was applied to the plantar surface of the paw for 3 s. A positive response resulted in application of a filament of lesser strength on the following trial, and no response in application of a stronger filament. To calculate the 50% withdrawal threshold, five responses surrounding the 50% threshold were obtained after the first change in response. The pattern of responses was used to calculate the 50% threshold = $(10[\chi+\kappa\delta])/10{,}000)$, where χ is the log of the final von Frey filament used, κ = tabular value for the pattern of responses and δ the mean difference between filaments used in log units. The log of the 50% threshold was used to calculate summary and test statistics, in accordance with Weber's Law.

Hargreaves' test

Spinal reflex responses to noxious heat stimulation were assessed using the Hargreaves' test.[90] Mice were habituated for an hour in plexiglass enclosures with a glass base. Before testing, the enclosures were cleaned of feces and urine. Radiant heat was then locally applied to the plantar surface of the hindpaw until the animal exhibited a nocifensive withdrawal response. Average latencies were obtained from three trials per animal, with inter-trial intervals of 15 min. Cut-off time was set to 30 s.

Cancer-induced bone pain

Cell culture

Lewis lung carcinoma (LL/2) cells (from American Type Culture Collection (ATCC)) were cultured in a medium containing 90% Dulbecco's Modified Eagle Medium (DMEM) and 10% fetal bovine serum (FBS) and 0.1% Penicillin/Streptomycin for 14 days before the surgery. DMEM was supplemented with L-glutamine (1%) and glucose (4.5 g/L). The cells were sub-cultured whenever ~80% confluency was reached, which was done a day before the surgery. On the surgery day, LL/2 cells were harvested by scraping and were centrifuged at a speed of 1500 rpm for 2 min. The supernatant was removed, and the cells were resuspended in a culture medium that contained DMEM to attain a final concentration of $\sim 2x10^6$ cells/ml. The cell counting and viability check were done using the Countess automated cell counter (Thermo Fisher Scientific).

Surgery

Surgery was carried out on anesthetized C57BL/6 mice. Anesthesia was achieved using 2–3% isoflurane. The legs and the thighs of the mice were shaved, and the shaved area was cleaned using hibiscrub solution. A sterile lacri-lube was applied to the eyes and

lidocaine was applied at the site of the surgery. The reflexes of the mice to pinches were checked to ensure successful anesthesia. An incision was made in the skin above and lateral to the patella on the left leg. The patella and the lateral retinaculum tendons were loosened to move the patella to the side and expose the distal femoral epiphysis. A 30G needle was used to drill a hole through the femur to permit access to the intramedullary space of the femur. The 30G needle was removed, and a 0.3mL insulin syringe was used to inoculate ~2x10^4 LL/2 cells suspended in DMEM. The hole in the distal femur was sealed using bone wax (Johnson & Johnson). To ensure that there was no bleeding, the wound was washed with sterile normal saline. Following that, the patella was placed back into its original location, and the skin was sutured using 6–0 absorbable vicryl rapid (Ethicon). Lidocaine was applied at the surgery site, and the animals were placed in the recovery chamber and monitored until they recovered.

Limb-use score

The mice housed in the same cage were placed together in a glass box (30 × 45 cm) for at least 5 min. Then each mouse was left in the glass box on its own and was observed for ~4 min, and the use of the ipsilateral limb was estimated using the standard limb use scoring system in which: 4 indicates a normal use of the affected limb; 3 denotes slight limping (slight preferential use of the contralateral limb when rearing); 2 indicates clear limping; 1 clear limping, and with a tendency of not using the affected limb; and 0 means there is no use of the affected limb. Reaching a limb-use score of zero was used as an endpoint for the experiment.

Static weight-bearing

The scale used for this behavioral test was the Incapacitance Meter (Linton Instrumentation), which has two scales to assess the weight put on each limb. The weight placed on each limb is measured for 3 s. The readings for the weight put on the limbs were recorded three times for each mouse, and between the readings, mice were allowed to re-place themselves into the tube. The fraction of the weight put on the ipsilateral paw was determined by the summation of all three readings of the weight put on the ipsilateral paw divided by the summation of all the weight measurements on both paws.

QUANTIFICATION AND STATISTICAL ANALYSIS

For behavioral experiments, *n* refers to the number of animals.

Details about the statistical and correlation analyses of RNA-Seqand the Quantitative RT-PCR data are detailed in the appropriate methods sections.

Datasets are presented using appropriate summary statistics as indicated in the figure legends. Error bars in all graphs denote mean ± SEM. Tests of statistical comparison for each dataset are described in detail in the figure legends. For grouped data, we made the appropriate correction for multiple comparisons. We set an α-value of $p = 0.05$ for significance testing and report all p values resulting from planned hypothesis testing, that are detailed for both main and supplemental figures in Tables S6 and S7, respectively.